Transposable element exaptation is the primary source of novelty in the primate gene regulatory landscape

Marco Trizzino[1,#,*], YoSon Park[1,*], Marcia Holsbach-Beltrame[1], Katherine Aracena[1], Katelyn Mika[2], Minal Caliskan[1], George H. Perry[3], Vincent J. Lynch[2] and Christopher D. Brown[1,#]

1. Department of Genetics, Perelman School of Medicine, University of Pennsylvania, Philadelphia, PA, 19104
2. Department of Human Genetics, University of Chicago, Chicago, IL, 60637
3. Departments of Anthropology and Biology, Pennsylvania State University, University Park, PA, 16802

* Co-first author
# Correspondence: chrbro@upenn.edu (C.D.B.), marco.trizzino83@gmail.com (M.T.)

Summary

Gene regulation plays a critical role in the evolution of phenotypic diversity. We investigated the evolution of liver promoters and enhancers in six primate species. We performed ChIP-seq for two histone modifications and RNA-seq to profile cis-regulatory element (CRE) activity and gene expression. The primate regulatory landscape is largely conserved across the lineage. Conserved CRE function is associated with sequence conservation, proximity to coding genes, cell type specificity of CRE function, and transcription factor binding. Newly evolved CREs are enriched in immune response and neurodevelopmental functions, while conserved CREs bind master regulators. Transposable elements (TEs) are the primary source of novelty in primate gene regulation. Newly evolved CREs are enriched in young TEs that affect gene expression. However, only 17% of conserved CREs overlap a TE, suggesting that target gene expression is under strong selection. Finally, we identified specific genomic features driving the functional recruitment of newly inserted TEs.

M.T. Current affiliation: Gene Expression and Regulation Program, The Wistar Institute, Philadelphia, PA, 19104

Introduction

The evolution of cis-regulatory elements (CREs) plays an important role in phenotypic and behavioral evolution (King and Wilson, 1975; Rockman et al., 2005; Loisel et al., 2006; Pollard et al., 2006; Prabhakar et al., 2008; Warner et al., 2009; Babbitt et al., 2010; Cain et al., 2011; Marnetto et al., 2014; Zhou et al., 2014; Villar et al., 2015). Many aspects of CRE evolution in mammals have been characterized (Schmidt et al., 2010; Cain et al., 2011; Zhou et al., 2014; Prescott et al., 2015; Reilly et al., 2015; Villar et al., 2015; Emera et al., 2016), and suggest a role for transposable elements (TEs) in the evolution of gene regulation (McClintock, 1950, 1984; Britten and Davidson, 1969; Davidson and Britten, 1979; Jordan et al., 2003; Bejerano et al., 2006; Wang et al., 2007; Bourque et al., 2008; Sasaki et al., 2008; Markljung et al., 2009; Kunarso et al., 2010; Lynch et al., 2011, 2015; Chuong et al., 2013, 2016; Schmidt et al., 2012; Xie et al., 2013; del Rosario et al., 2014; Sundaram et al., 2014; Du et al., 2016; Rayan et al., 2016). However, validating the functional contribution of TEs in the mammalian gene regulation remains a challenge. Lynch et al. (2011, 2015) demonstrated that the recruitment of novel regulatory networks in the uterus was likely mediated by ancient mammalian TEs. However, Emera and colleagues (2016) suggested that neocortical enhancers do not exhibit strong evidence of transposon exaptation.

Many important questions remain unanswered: to what extent are poised and active regulatory elements functionally conserved? Are specific genomic features predictive of CRE conservation? To what extent have TEs driven the evolution of gene regulation? And finally, what determines which TE insertions are recruited as functional CREs? Establishing answers to these questions is critical for understanding how the evolution of regulatory elements contributes to the conservation and divergence of gene expression and complex traits.

With a goal of answering these questions, we collected liver samples from six primate species. Core liver functions are largely conserved across primate species. However, different environmental exposures, diets, and lifestyles likely directed the adaptation of liver functions, and associated regulatory evolution, making this tissue an optimal model in which explore the conservation and divergence of the gene regulation.

To characterize primate liver cis-regulatory evolution, we performed chromatin immunoprecipitation followed by sequencing (ChIP-seq) for Histone H3 Lysine 27

acetylation (H3K27ac), which marks active enhancers and promoters, and Histone H3 Lysine 4 mono-methylation (H3K4me1), which marks poised regulatory elements on liver tissues from six primate species, including at least one species from each major primate clade to maximize evolutionary diversity within primates (Perelman et al., 2012). We generated whole transcriptome sequencing (RNA-seq) data from the same specimens to quantify gene expression variation across species. We estimated the degree of evolutionary conservation of regulatory activity and gene expression levels across the entire lineage, and characterized the genomic features associated with evolutionary conservation of gene regulation, to understand why some enhancers and promoters are conserved across species whereas others are subject to rapid turnover.

The activity of the majority of human CREs is conserved across the entire primate lineage, and the differences in gene expression and regulation reflect the phylogenetic distance between species. Conservation of cis-regulatory activity is associated with nucleotide sequence conservation, gene function, gene distance, cell-specificity of CRE function, and transcription factor binding site (TFBS) density. Strikingly, human- and ape-specific enhancers and promoters are significantly enriched for evolutionarily young TEs. In particular, the majority of human- and ape-specific CREs are derived from SINE-VNTR-*Alus* (SVAs) and Long-Terminal-Repeats (LTRs), respectively. On the other hand, only a minor fraction of evolutionarily conserved CREs are derived from TEs, indicating that purifying selection on the associated genes likely preserve these CREs from being disrupted by TE insertions, thus conserving the expression of the associated genes. In addition, we characterized SVAs that evolved into regulatory elements, and estimated potential impacts of these SVAs on gene regulation across the lineage. We validated the regulatory activity of several TE families, and conclude with a new model describing specific genomic features that strengthen the potential adaptation of TEs into functional regulatory elements (exaptation; Brosius and Gould; 1992; de Souza et al., 2013).

Results

Data generation, quality assessment, and validation

We generated a total of 757 million RNA-seq reads and 1.70 billion ChIP-seq reads (H3K27ac, H3K4me1, and input) from *post mortem* livers of three or four individuals per

species of mouse lemur (*Microcebus murinus*), bushbaby (*Otolemur garnettii*), marmoset (*Callithrix jacchus*), rhesus macaque (*Macaca mulatta*), chimpanzee (*Pan troglodytes*), and human (*Homo sapiens*) (Fig. 1; Table S1). The six species were selected to include at least one species from each of the major primate clades, thus maximizing phylogenetic diversity within primates. The samples were all from young adults and, with the exception of the bushbaby, included both males and females. In total, 18 RNA-seq and 14 ChIP-seq samples remained post-QC and were used for analyses (Table S1). On average, we sequenced 42.1 million RNA-seq reads and 40.6 million ChIP-seq reads per sample (Table S1). We applied stringent quality control (QC) measures to assess library construction, sequencing, and peak-calling methods. Read mappability after the filtering steps was consistent across species and assays (77% in ChIP-seq, 78% in RNA-seq; Table S1), suggesting that differences in genome assembly quality do not introduce large biases.

ChIP-seq data were used to map the distribution of active (H3K27ac) and poised (H3K4me1) CREs in the six primate genomes (Fig. 1). We mapped ChIP-seq reads to their respective reference genomes with BWA-mem (Li, 2013) and identified regions of significant H3K27ac and H3K4me1 enrichment in the human liver, treating all human individuals as replicates in the peak calling procedure with MACS2 (Zhang et al., 2008). 85.6% of the regions marked by H3K4me1 overlapped regions marked by H3K27ac. A total of 84,253 human peaks remained after merging overlapping peaks from the two histone markers. Next we identified regions orthologous to the human consensus peaks from the genomes of non-human primates using the Ensembl multiple sequence alignment (MSA) database. We catalogued 47,673 total human CREs with orthologs in all six species: 40,527 enhancers (distance from transcription start site (TSS) > 1 kb) and 7,146 promoters (distance from TSS ≤ 1 kb).

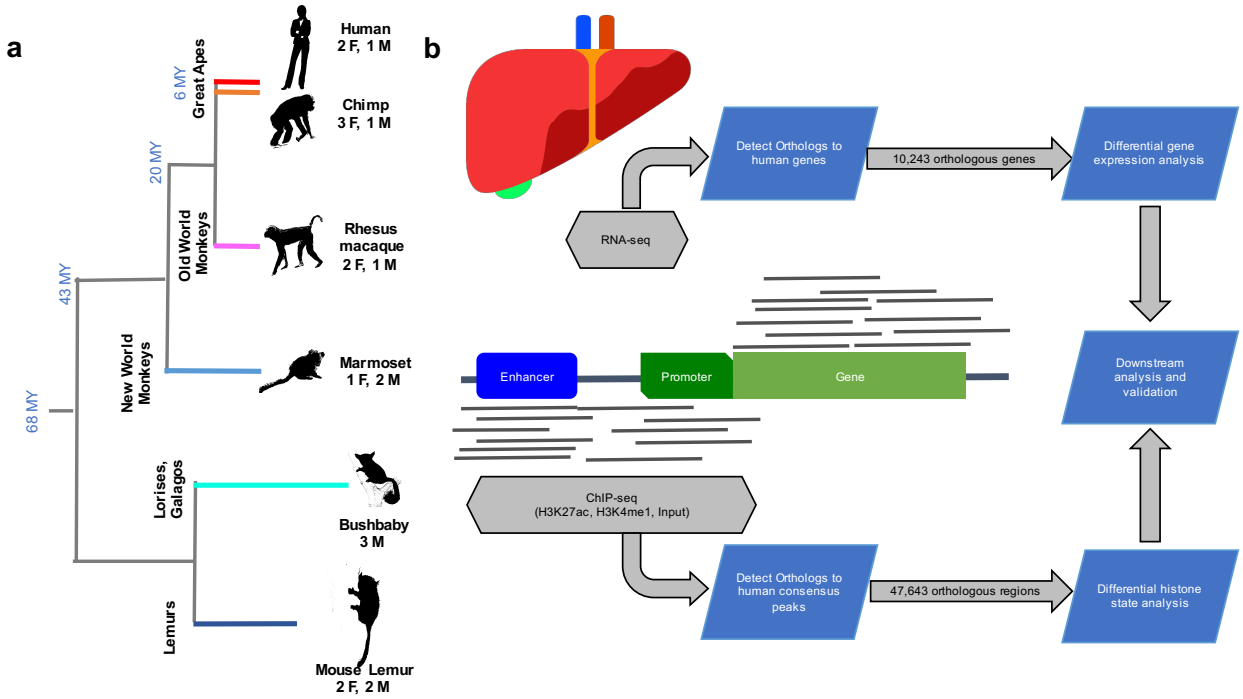

Figure 1 - **Experimental design and analytical pipeline**. (A) Sampling included three to four specimens from six species representing all of the major primate clades. (B) ChIP-seq and RNA-seq profiles were produced from the liver samples. Differential histone modification and gene expression analyses were performed on the orthologous CREs and genes in each species, respectively. Outputs shown in the diagram were used for downstream analyses and validations.

Several lines of evidence indicate that the regions of histone modification we have identified represent active CREs. First, 99.0% and 73.3% of ENCODE HepG2 H3K27ac and H3K4me1 regions (ENCODE Project Consortium, 2012), respectively, overlapped with one or more human peaks. Similarly, 63.2% of the 43,011 permissive enhancers that were predicted by the FANTOM5 Consortium based on enhancer RNA expression (Andersson et al., 2014) overlapped with one or more of human peaks identified in our study. Further, the promoters of 98.1% of genes expressed in the liver overlapped a region of histone modification (Fig. S1). Finally we compared our human H3K27ac data to a recent study focused on liver CREs in mammals (Villar et al., 2015) and demonstrated that peaks bearing signatures of robust and broad regulatory activities are largely reproducible across studies, despite variation attributable to different study designs (Fig. S2).

ChIP-seq experiments can identify regions of the genome bound by histones and other proteins that characterize regulatory elements, however, this does not guarantee

144 these regions are functional regulatory elements (Pickrell et al., 2011; Cusanovic et al.,
145 2014; Jain et al., 2015). Therefore, we used a novel parallelized reporter assay (Melnikov et
146 al., 2012; Patwardhan et al., 2012; Sharon et al., 2012; see methods) to validate the
147 regulatory function of predicted human liver CREs. Specifically, we tested the regulatory
148 activity of 1 kb fragments from 122 putative regulatory elements in HepG2 cells, including
149 both evolutionarily conserved and recently evolved CREs (see below). Among 122 tested
150 elements, 79 drove significant reporter gene expression levels (42/53 enhancers [79.2%]
151 and 36/69 promoters [52.2%]; Table S6), suggesting that the majority of the CREs
152 predicted in our study based on the enrichment of active histone modification states are
153 likely functional regulatory elements in the human liver.
154
155 **The majority of human CREs are functionally conserved across primates**
156 After extracting ChIP-seq read counts for the six species from 47,673 orthologous regions,
157 we assessed evidence of differential histone modification between species with DESeq2
158 (Love et al., 2014), using the ChIP-seq input data as a covariate. We compared ChIP-seq
159 read counts in the 47,673 regions by means of all possible human-centric species × species
160 and group × group pairwise comparisons (see methods). This approach provides a
161 quantitative assessment of histone modification profiles across species, while avoiding
162 issues arising from many potential experimental variables that may confound peak calling
163 (Waszak et al., 2015). A specific analysis of human and marmoset, the latter being the
164 species with the smallest number of peaks called in this study (Supplemental File S1),
165 strongly supported the validity and robustness of our approach (Fig. S3).
166 The majority of the 47,673 human CREs (63.8%) did not show significant differential
167 histone modifications in any of the tested pairwise comparisons (FDR < 10%; Fig. 2). This
168 suggests that these regulatory regions are consistently active across the primate lineage
169 and thus represent evolutionarily conserved primate CREs. Although the absence of
170 differential histone modifications in a pairwise comparison between two species is not a
171 direct proof of CRE conservation, we demonstrated that the selected FDR threshold does
172 not affect downstream conclusions (Table S7). As an additional control, we performed a
173 chimpanzee-centric analysis for the regions orthologous to chimpanzee consensus peaks
174 (hereafter, chimpanzee CREs), and demonstrated that 62.5% of these regions were not
175 differentially histone modified in any of the pairwise comparisons. This observation is
176 consistent with 63.8% conserved CREs identified in the human-centric analysis, indicating

177 that the differential histone modification analysis is robust and species-specific bias is
178 unlikely.

179 Promoters are significantly more conserved than enhancers (68.9% and 62.8%,
180 respectively; Fisher's exact test $p < 2.2\times10^{-16}$; Fig. 2), as observed previously (Villar et al.,
181 2015). On the other hand, 36.2% of orthologous CREs exhibited differential histone
182 modification state across species (Fig. 2). We detected 57 human-specific CREs (0.13%;
183 Fig. 3) and 544 ape-specific CREs (1.42%; Fig. 3). Together, our differential histone state
184 analysis results are broadly supported by several studies that have consistently suggested
185 a high degree of regulatory element conservation between closely related species in
186 metazoans (Cotney et al., 2013; Boyle et al., 2014; Prescott et al., 2015; Reilly et al., 2015;
187 Emera et al., 2016).

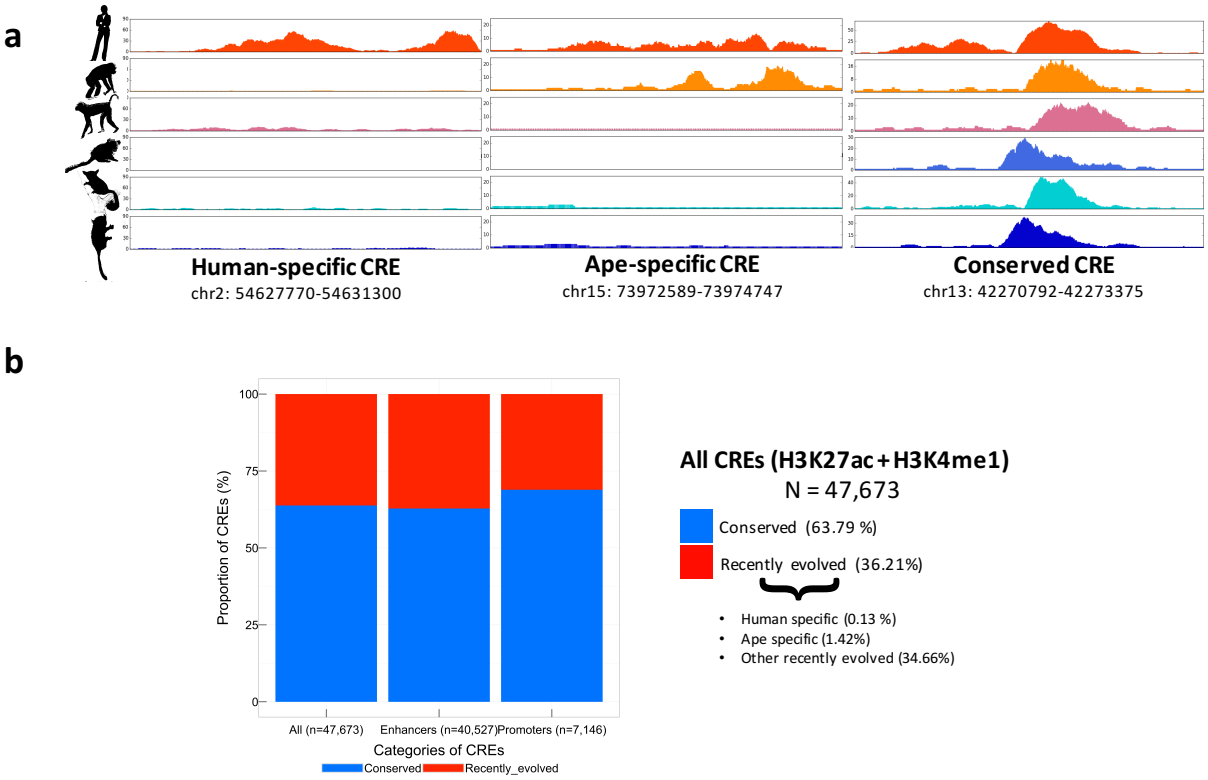

188

189 **Figure 2 - Primates CREs are evolutionarily conserved**. (A) Plots show examples of
190 human-specific, ape-specific and conserved CREs. (B) Fractions of conserved and recently
191 evolved primate CREs, with breakdown of enhancers and promoters.
192

193 Next, we assessed the extent to which primate-conserved CREs identified in this
194 study are also evolutionarily conserved across a broader range of mammals. In particular,
195 we compared our conserved H3K27ac CREs with the H3K27ac profile of the opossum, the
196 species with the earliest divergence from humans (>180 million years) in the Villar et al.

(2015) dataset. 2,854 primate-conserved promoters and 9,456 primate-conserved enhancers have orthologous regions in the opossum genome. Among these, 71.3% of the promoters and 19.1% of the enhancers had significant H3K27ac enrichment in both species, supporting that most of the primate conserved promoters show conserved activity in all of the mammalian clade, whereas only a fraction of the primate conserved enhancers is also conserved across mammals. Further, the two studies come to consistent estimates of the fraction of differentially active CREs per million years: 0.06–0.12% in primates and 0.07% in mammals.

The conservation of the nucleotide sequence is associated with conservation of regulatory activity

Previous studies have suggested that the sequence conservation is associated with conservation of regulatory activity, especially in absence of comparative functional assays (Brown et al., 2007; Cooper and Brown, 2008; Pollard et al., 2010; Gittelman et al., 2015; Holloway et al., 2015; Villar et al., 2015; Yang et al., 2015; Dong et al., 2016; Lewis at al., 2016). For each human-centric species × species comparison, we estimated: i) the fraction of differentially modified CREs; ii) the fraction of differentially expressed genes from a set of 10,243 genes with six way orthologs (Table S3); and iii) the per-nucleotide pairwise sequence divergence for each species with respect to humans for each of the 47,673 unique orthologous CREs

Differential histone state fractions ranged from 0.77% in the human × chimpanzee, to 21.9% in the human × mouse lemur comparisons (Fig. 3a). Similarly, differential gene expression ranged from 5.93% in the human × chimpanzee to 16.0% in the human × mouse lemur comparisons (Fig. 3b). Both differential histone modification and differential gene expression fractions reflected phylogenetic distance between humans and other tested species. Differentially expressed genes were significantly more likely to be associated with a differentially modified CRE than expected by chance (9.90%; Fisher's exact test $p < 2.2\times10^{-16}$).

Sequence conservation was significantly correlated with regulatory activity (human × chimpanzee, logistic regression $p = 5.7\times10^{-16}$; human × rhesus macaque, $p = 6.7\times10^{-8}$; human × marmoset, $p = 4.0\times10^{-9}$; human × bushbaby, $p < 2.2\times10^{-16}$; human × mouse lemur, $p < 2.2\times10^{-16}$; Fig. 3c). 24,691 CREs overlapped 94,578 placental mammal phastCons elements (i.e. regions of the genomes with consistent nucleotide sequence conservation across species; Siepel et al., 2005). The fraction of evolutionary conserved

231 CREs overlapping these conserved elements was higher than expected by chance
232 (Fisher's exact test $p < 2.2\times10^{-16}$). Together, these data demonstrate that CREs with
233 conserved nucleotide sequence are significantly more likely to have conserved regulatory
234 activity and are associated with conserved gene expression.
235

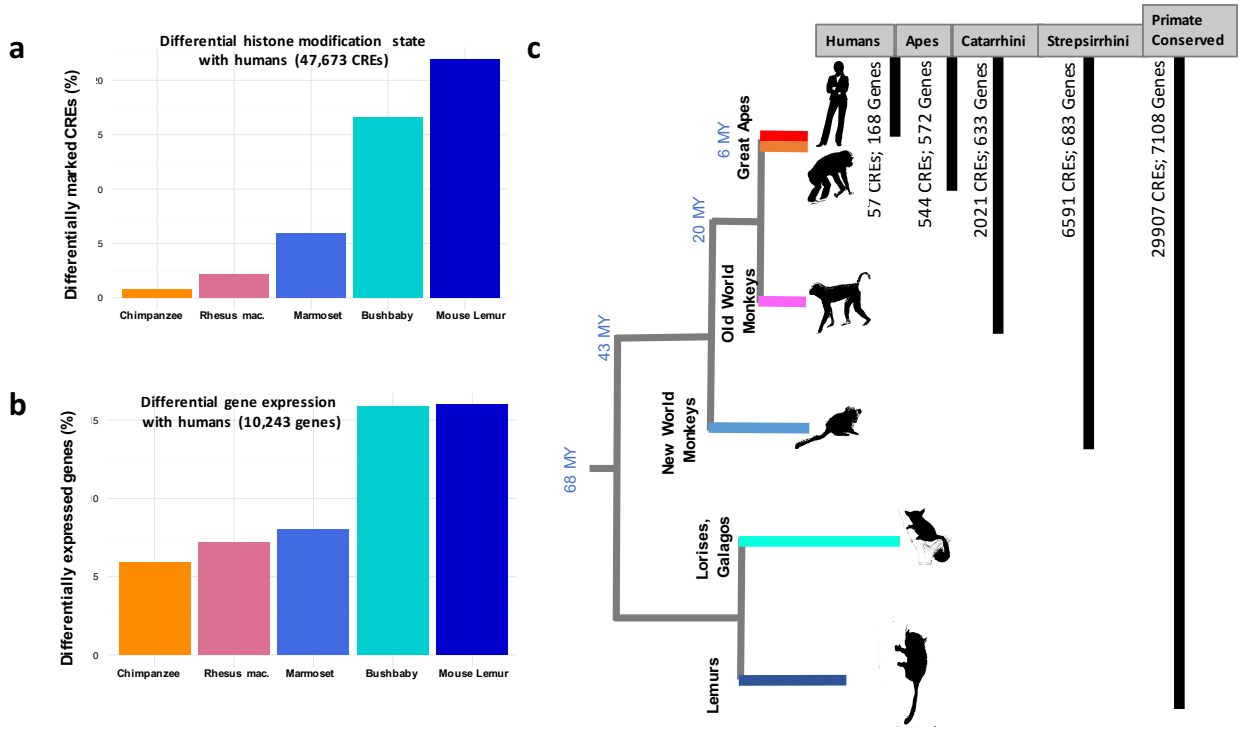

236

237 **Figure 3 - Differential histone mark and gene expression across species**. (A) Human-
238 centric pairwise comparisons for differential histone modification states on 47,673
239 orthologous CREs. (B) Human-centric pairwise comparisons for differential gene
240 expression of 10,243 orthologous CREs. (C) Number of lineage-specific CREs (i.e. CREs
241 significantly more active in each lineage compared to other primates) and genes (i.e. genes
242 upregulated in each lineage compared with other primates) in the primate phylogeny.
243

244 **Genomic features associated with CRE conservation and rapid evolution**

245 To understand the mechanisms responsible for CRE conservation and turnover, we
246 identified genomic features associated with conserved regulatory activity. CREs associated
247 with protein coding genes were significantly more conserved than CREs associated with
248 either pseudogenes (Fisher's exact test $p = 3.3\times10^{-3}$) or lincRNAs (Fisher's exact test $p =$
249 5.2×10^{-7}; Fig. 4a). For closely related species, regulatory activity was conserved, regardless
250 of the distance to the nearest TSS (human × chimpanzee, logistic regression $p = 0.261$;
251 human × rhesus macaque, $p = 0.336$; Fig. 4b). However, for more distantly related species
252 pairs, the evolutionary conservation of the CRE activity was significantly lower in regions

253 more distant from TSSs (human × marmoset, logistic regression $p = 6.0\times10^{-15}$; human ×
254 bushbaby, $p = 2.1\times10^{-5}$, human × mouse lemur, $p = 2.8\times10^{-5}$; Fig. 4b). Intronic enhancers
255 were significantly more conserved than intergenic enhancers (63.0% and 55.2%
256 respectively; Fisher's exact test $p < 2.2\times10^{-16}$). These data demonstrate increased selective
257 pressure to maintain regulatory activity in the vicinity of protein coding genes.

258 Multiple genomic features indicative of broad regulatory element activity were
259 significantly associated with the conservation of regulatory activity across the primate
260 phylogeny. Promoters and enhancers overlapping regions of chromatin accessibility in
261 many cell types (ENCODE Project Consortium, 2012) were significantly more functionally
262 conserved than those that are functional in only a small number of tissues (logistic
263 regression $p < 2.2\times10^{-16}$; Fig. 4c). Similarly, CREs that overlapped many TFBS, as
264 identified by ENCODE ChIP-seq in HepG2 cells, were significantly more evolutionarily
265 conserved than those with fewer binding sites (logistic regression $p < 2.2\times10^{-16}$; Fig. 4d).
266 Further, liver enhancers that generate consistent enhancer RNA transcription were
267 significantly more evolutionarily conserved than the untranscribed enhancers (Fig. S3;
268 Fisher's exact test $p = 0.04613$), validating previous findings (Andersson et al., 2014).

269 Finally, we used GOrilla (Eden et al., 2007; Eden et al., 2009) to identify biological
270 processes Gene Ontology terms that are enriched in genes found within 10-kb of
271 evolutionarily conserved CREs, using as background all of the genes found within 10 kb
272 from any of the 47,673 orthologous CREs. We found an enrichment for housekeeping
273 functions involved in the regulation of cellular, transcriptional and developmental processes
274 (Table S4). These findings support previous observations that conserved CREs are
275 proximal to housekeeping genes (FANTOM5 Consortium, 2014; Villar et al., 2015).
276

277 **Specific transcription factor motifs are associated with regulatory conservation and**
278 **turnover**

279 We used the MEME Suite (Bailey et al., 2009) to identify sequence motifs enriched in
280 human-specific, ape-specific, and evolutionarily conserved liver CREs. Human-specific
281 CREs were enriched with motifs for TFs associated with immune response and
282 hematopoietic maintenance (Fig. 4e; Supplemental File S2), such as PRDM1 (BLIMP1)
283 which is induced upon viral infection and represses beta-interferon (β-IFN) gene
284 expression. The rapid evolution of immune response genes and TFs is supported by many
285 studies in vertebrates and in *Drosophila melanogaster*, demonstrating that while the central
286 machinery of immune responses is strongly conserved, several components of the

287 extended molecular networks can evolve rapidly or diversify as a consequence of
288 evolutionary competition between hosts and pathogens (Jansa et al., 2003; Vallender 2004;
289 Sackton et al., 2007; Obbard et al., 2009; Schadt et al., 2009; Grueber et al., 2014; Lazzaro
290 and Schneider 2014; Salazar-Jaramillo et al., 2014; Zak et al., 2014; Sironi et al., 2015;
291 Wertheim, 2015; Chuong et al., 2016). Similarly, recently evolved promoters and enhancers
292 in primates are enriched in functions associated to neuronal proliferation, migration and
293 cortical map organization (Boyd et al., 2015; Reilly et al., 2015; Emera et al., 2016). In
294 contrast, ape-specific CREs were instead enriched with motifs representing binding sites for
295 TFs involved in liver function but, remarkably, also in brain and neural system proliferation
296 and development (Fig. 4e; Supplemental File S2).

297 Evolutionarily conserved CREs were enriched in TFBSs for master regulators and
298 homeobox genes that establish cell-type identity in liver cells (Fig. 4e; Supplemental File
299 S2). Among these master regulators, HNF4A is essential for the differentiation of human
300 hepatic progenitor cells by establishing the expression of the network of transcription
301 factors that controls the onset of hepatocyte cell fate (DeLaForest et al., 2011). Likewise,
302 CEBPA is required for the liver cell specification and gene function, and the associated
303 TFBSs are highly conserved across mammals (Ballester et al., 2014). Both CEBPA and
304 HNF4A have conserved cis-regulatory activity and significantly higher numbers of shared
305 TF binding events than expected by chance alone across distant vertebrates (Schmidt et
306 al., 2010). These results demonstrate that evolution shapes the regulatory landscape by
307 preserving the regulatory activity in essential metabolic and developmental pathways, while
308 permitting incessant renovation of specific networks that are under strong selective
309 pressures.

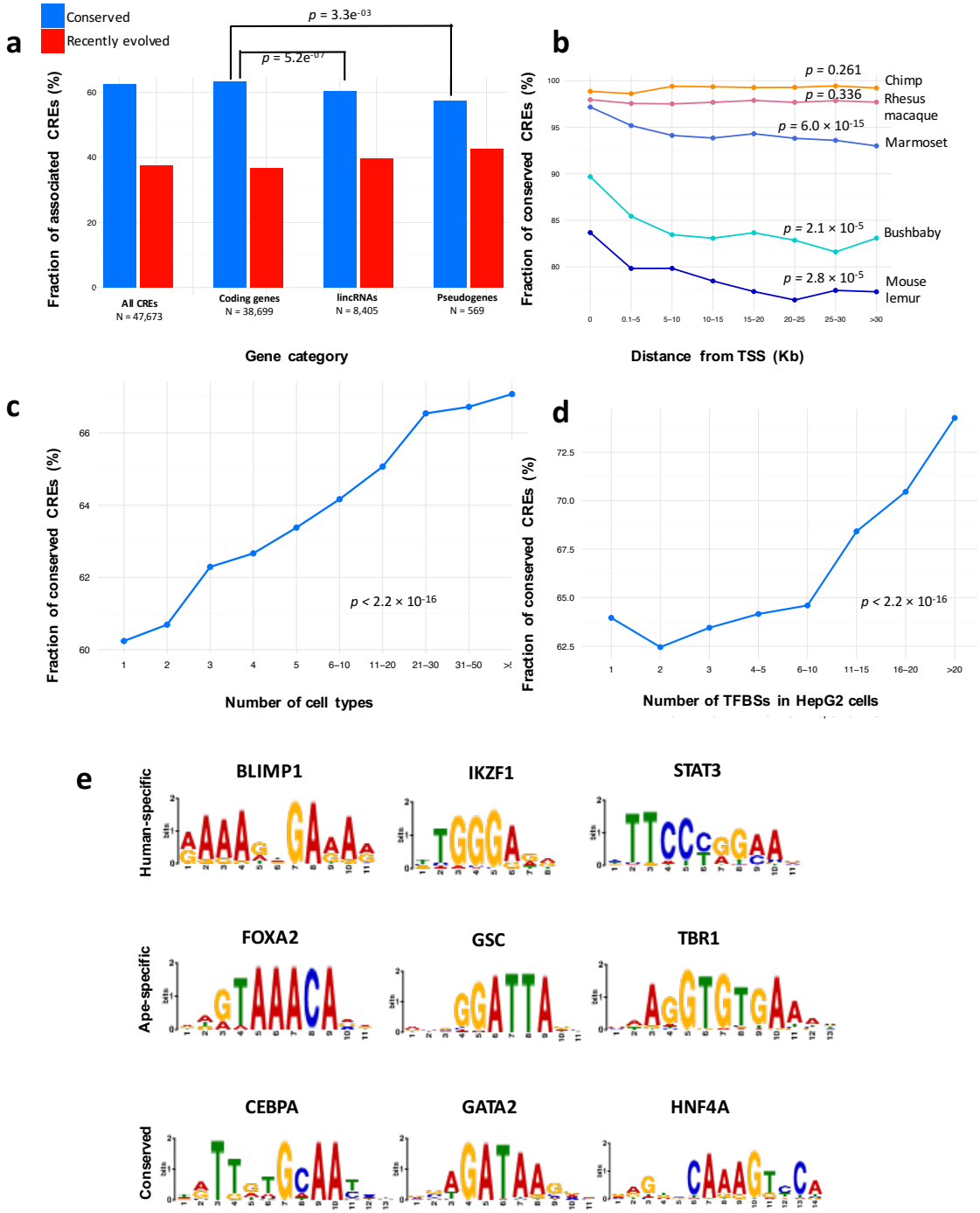

Figure 4 - Genomic features associated to CRE conservation. (A) Fractions of conserved and recently evolved CREs associated to protein coding genes, lincRNAs and pseudogenes. (B) Distribution of CRE conservation along the genome. (C) Correlation between CRE conservation and cell-type specificity based on ENCODE data. (D) Correlation between CRE conservation and number of ENCODE HepG2 TFBSs present of each CRE. (E) Examples of i) enriched motifs associated to immune response (BLIMP1, IZKF1, STAT3) in human-specific CREs; ii) enriched motifs associated to language and neural development (FOXA2, GSC, TBR1) in ape-specific CREs; iii) enriched motifs associated to master regulators (CEPBA, GATA2, HNF4A) in conserved CREs.

320 **Exaptation of TEs into functional CREs is pervasive in the primate genomes**
321 Previous studies have found that TEs can contribute to the origin of CREs. To quantify the
322 contribution of TEs in the liver gene expression regulation in primates, we annotated each
323 liver CRE based on overlap with RepeatMasker elements (Smit, Hubley & Green, 2013-
324 2015; http://www.repeatmasker.org). We found that 28.7% of human liver CREs overlapped
325 an annotated TE, most of which were SINEs (59.8% of the total) and LINEs (21.2%),
326 although LTRs (9.3%) and DNA transposons (8.4%) were also abundant. 27 TE families
327 were significantly enriched within the set of 47,673 orthologous CREs (FDR < 1%), nearly
328 all of which were SINE-VNTR-*Alu*s (SVAs), LTRs, and *Alus* (Figure 5), suggesting these
329 TEs contributed to the regulatory landscape in the primate liver (Jordan et al., 2003;
330 Schmidt et al., 2012; Sundaram et al., 2014; Lynch et al., 2015).
331 The majority (75.0%) of the enriched TE families were relatively young, and specific
332 to humans (SVA-F), Hominidae (SVA-B, SVA-C, and SVA-D), Hominoidea (the LTR12
333 subfamily), Simiiformes (LTRs), or primates (Alu elements), whereas the remaining 25.0%
334 were Eutherian-specific or older (Fig. 5, Fig. S7, and Table S5). We therefore investigated
335 whether these recent TE insertions altered the expression patterns of nearby genes in
336 primates. Specifically, we focused on the enriched TE families younger than the
337 Strepsirrhini/Haplorrhini divergence, thus not present in mouse lemur and bushbaby. We
338 found that 22.6% of the CREs overlapping SVAs, and 12.5% of the CREs overlapping LTRs
339 were differentially expressed between the Strepsirrhini (human, chimpanzee, rhesus
340 macaque and marmoset) and the Haplorrhini (mouse lemur and bushbaby). Both of these
341 fractions were significantly higher than expected by chance (binomial test $p < 2.2\times10^{-16}$).
342 Together, these findings indicate that TEs have played a key role in shaping primate gene
343 regulation, introducing novel gene expression patterns as a consequence of their
344 recruitment as functional CREs.
345
346 **The vast majority of newly evolved CREs are derived from TE insertions**
347 84.2% of ape-specific CREs and 94.7% of human-specific CREs overlap at least one TE
348 (Fig. 5; Fig. S7). In contrast, only 17.0% of evolutionarily conserved CREs contain an
349 annotated TE (Fisher's exact test $p < 2.2\times10^{-16}$). However, we hypothesize that this may be
350 an underestimate due to the inability to recognize ancient TE insertions accumulating
351 mutations over time. LTRs and SVAs were the most frequently exapted TEs in newly
352 evolved CREs (LTR = 40.1% of the exapted TEs in ape-specific CREs; SVA = 75.3% of the
353 exapted TEs in the human-specific CREs; Fig. 5), despite being among the least common

classes of repeats in the human genome (15.9% and 0.69% of the total TEs respectively; Fisher's exact test $p < 2.2\times10^{-16}$ for both of the TE categories).

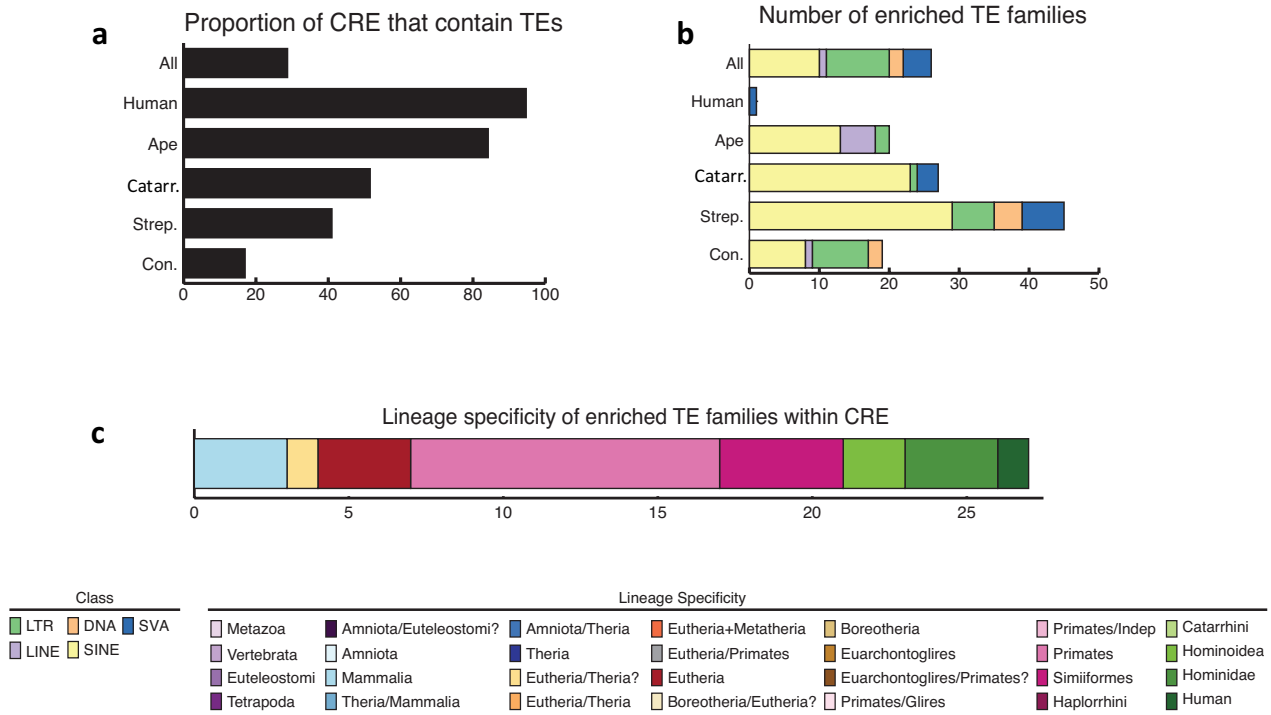

Figure 5 - **Newly evolved CREs are enriched in TEs**. (A) Proportion of CREs that overlap TEs in the different primate lineages. (B) Number of enriched TE families within CREs in the different primate lineages. (C) Most enriched TE families in primates.

The contribution of LTRs in primate gene regulation has been characterized in previous studies (Wang et al., 2007; Cohen et al., 2009; Sundaram et al., 2014; Janoušek et al., 2016). In our data, a remarkable example of an ape-specific CRE derived from LTR insertion is an enhancer at the gene *GRIN3A*. This gene is involved in physiological and pathological processes in the central nervous system and has been associated with several complex human diseases, including schizophrenia (Takata et al., 2013). Our differential histone modification analysis identified an ape-specific ChIP-seq peak overlapping a 1-Kb long ape-specific insertion (present also in orangutan and gorilla, but not in other primates; GRCh38 chr9:101,723,127-101,724,197). This insertion, located 13 Kb from the TSS of *GRIN3A*, is entirely derived from an LTR-12C. The insertion drove strong enhancer activity upon transfection into HepG2 cells (Wilcoxon's rank sum test p = 0.00017; Fig. S5), suggesting that the transposable element was recruited as functional enhancer in the *GRIN3A* locus.

374 SVAs are instead a hominid-specific family of composite retrotransposons that are
375 active in humans (Hancks and Kazazian, 2010), with more than 3,500 annotated copies.
376 Given that nearly all human-specific liver CREs were derived from SVA insertions in our
377 analysis, we further investigated the genomic features of SVA insertions that lead to
378 exaptation (Table S5). 49.5% of human SVAs overlapped regions of significant histone
379 modification, and 97.8% of those were enhancers. These exapted SVAs are significantly
380 more likely to be associated with protein coding genes than the non-exapted SVAs (Fisher's
381 exact test p = 0.017) and are significantly closer to the TSS of the associated gene (mean
382 of 52.9 kb versus 64.1 kb; Wilcoxon rank-sum test $p < 2.2\times10^{-16}$). Exapted and non-exapted
383 SVAs lie within open chromatin regions in approximately the same number of cell types
384 (3.44 and 3.94 respectively; logistic regression p = 0.827) and host on average a
385 comparable density of TFBSs (3.28 and 1.95; logistic regression p = 0.679). However,
386 exapted SVAs have a significantly higher number of TFBSs in the neighboring regions (8.12
387 versus 5.86 in +/- 10kb; logistic regression $p = 1.91\times10^{-5}$). Taken together, these data
388 suggest a model where an SVA has a higher probability of becoming a CRE if it inserts in
389 TFBS-dense regions near protein coding gene promoters. (Fig. 6).
390 Among the exapted SVAs, our data predicted an intronic CRE for the gene *JARID2.*
391 This gene is an accessory component of Polycomb Repressive Complex-2 (PRC2), recruits
392 PRC2 to chromatin, and is involved in liver, brain, neural tube development, and embryonic
393 stem cell differentiation (Kaneko et al., 2014). Our differential histone state analysis
394 revealed a human-specific ChIP-seq peak overlapping a human-specific 1.9 kb-long
395 insertion, entirely derived from an SVA-F retrotransposon. JARID2 is significantly
396 downregulated in humans compared to all the other primates (Benjamini–Hochberg p =
397 0.019). Exapted SVAs-Fs exhibit significant enrichment for binding sites of known
398 transcriptional repressors such as PAX-5, FEV, and SREBF1 (Maurer et al., 2003; Fazio et
399 al., 2008; Lecomte et al., 2010). Indeed, the JARID2 SVA-F insertion leads to significantly
400 decreased expression in HepG2 reporter assays (Wilcoxon's rank sum test p = 0.00275;
401 Fig. S6), supporting the role of this SVA-F as a transcriptional repressor.
402

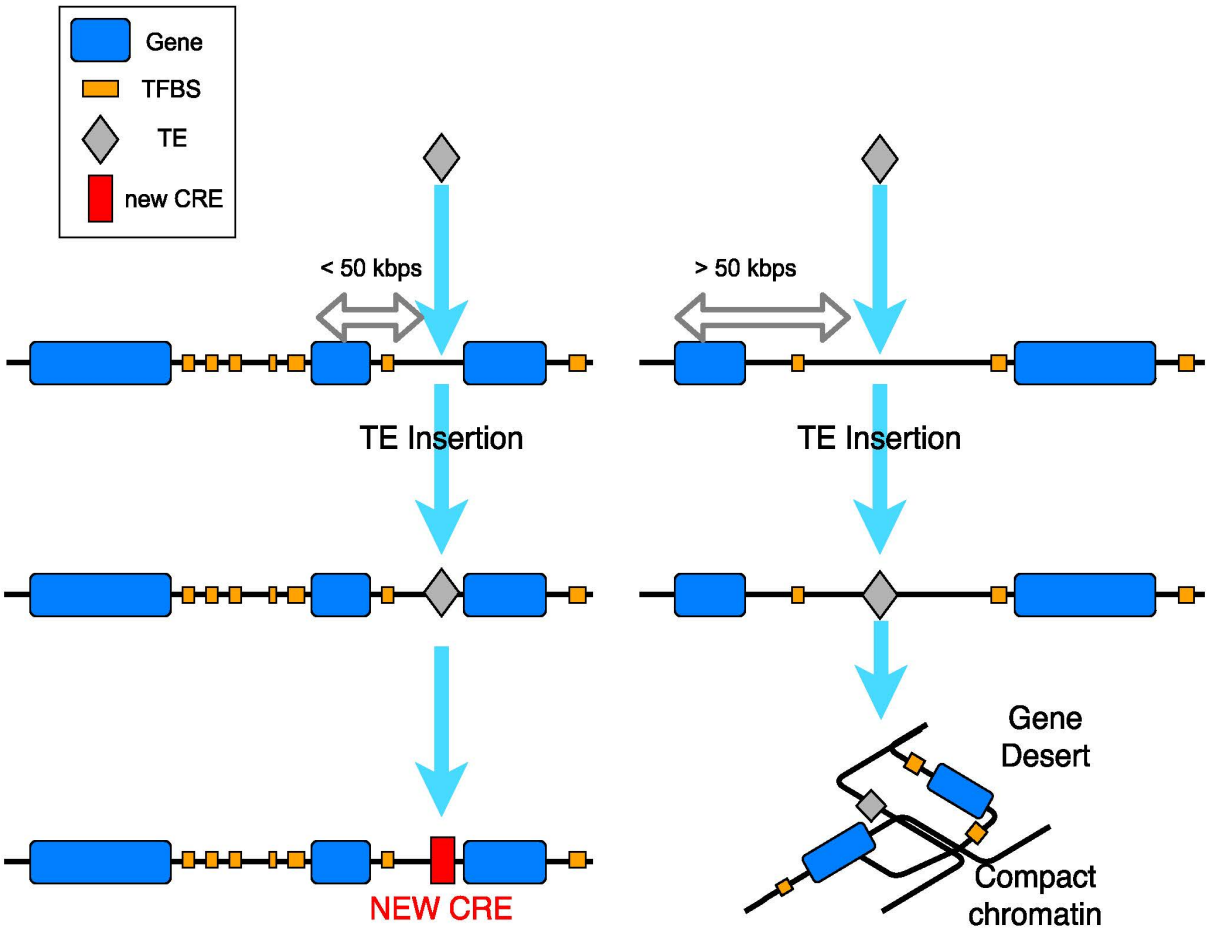

Figure 6 - **Model for exaptation of SVAs into human functional CREs**. A given SVA has a higher probability of being recruited as a functional cis-regulatory element if it is found within 50 kb from a protein coding gene, in a genomic region already enriched in TF binding motifs in the surrounding 10 kb up- and downstream.

Broad regulatory activity of TE insertions in the primate liver

Our findings strongly suggest that the majority of novel CREs in primates is derived from TE insertions. To validate the predicted regulatory activity of recent TE insertions, we tested the cis-regulatory activity of 69 TE subfamilies, covering all of the main classes and families of TEs (Table S6). TEs from these families overlap 3,897 of our predicted CREs. We synthesized the mammalian consensus sequence (see experimental procedures) for 69 different TE families, cloned them into a luciferase reporter vector with a minimal promoter, and transfected them into HepG2 cells to perform dual luciferase reporter assays. We found that luciferase expression for 66 of the 69 (95.6%) tested TE families was significantly different from the negative control (Fig. 7a; Wilcoxon's rank sum test p-values in Table S6). Strikingly, only 17 (25.7%) of these, mostly LTRs and DNA transposons, produced activity

significantly higher than the negative control (Fig. 7a), whereas the remaining 49 (74.3%), mostly LINEs, repressed transcription. Consistent with results from the JARID2 locus presented above, SVA-Fs were confirmed to function as transcriptional repressors.

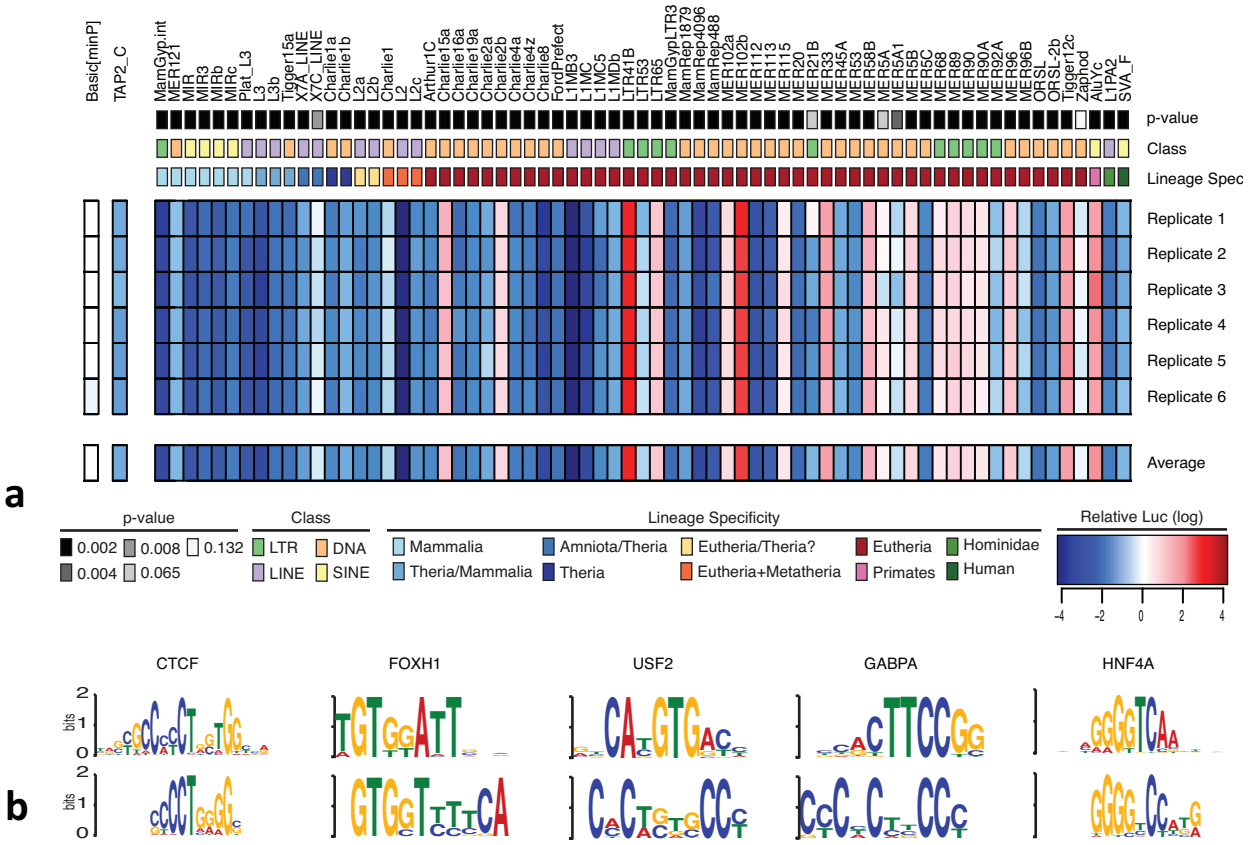

Figure 7 - Regulatory ability of TE families found in poised and active regulatory elements in HepG2 cells. (A) The p-value, class, and lineage specificity for the 69 TE families tested in HepG2 cells for regulatory ability, the empty vector control (Basic[minP]), and the positive control (TAP2_C) are all shown above the 6 luciferase assay replicates conducted and the average regulatory ability found across the replicates. Red indicates luciferase expression higher than the empty vector control; blue indicates luciferase expression less than Basic[minP]. (B) CTCF, FOX, USF2, GABP, and HNF4a binding motifs were found to be enriched in the sequences of the 66 TE families that drive expression significantly different from background. The top row shows the enriched sequence found while the bottom shows the Jaspar binding motifs recognized for each transcription factor.

These findings support that LTRs, among the most enriched TEs in our peak set, and the most common exapted TEs in apes, are likely co-opted as active enhancer elements. The putative repressor activity of LINEs is consistent with their underrepresentation in the human ChIP-seq peak set. However, we hypothesize that, at least for some of the TE families, such observed repressing activity levels could be the

442 byproduct of secondary biological mechanisms leading the cell to recognize these elements
443 as newly inserted TEs, and therefore silencing them via epigenetic mechanisms. However,
444 further tests will be needed to support this hypothesis.
445 The consensus sequences for the 66 TEs that drove reporter expression significantly
446 different from background were analyzed with MEME to identify enriched motifs. Motifs for
447 known master regulators of liver cell identity, including FOX, USF2, GABP, and HNF4A
448 (Wallerman et al., 2009), were significantly enriched within the sequences of the 66 TE
449 families with significant regulatory activity (Fig. 7b). In summary, most TE families function
450 as CREs in the primate liver, either as strong enhancers or as repressors. TEs are actively
451 recruited into the regulatory landscape, further supporting our findings on the pervasive
452 involvement of TEs in the primate gene regulation.
453

454 ## Discussion

455

456 **The primate regulatory landscape is evolutionarily conserved**

457 Only a small fraction (<1.50%) of the CREs were differentially active between humans and
458 chimpanzees. This suggests that even modest changes in gene regulation produce
459 observable phenotypic differentiation, and confirm that cis-regulatory evolution plays a
460 central role in primate diversification (Davidson 2001, 2006; Wray, 2007; Ho et al., 2009;
461 Tsankov et al., 2010; Smith et al., 2013; Martin et al., 2012; Coolon et al., 2014; Martin and
462 Reed, 2014; Guo et al., 2015; Lynch et al., 2015; Villar et al., 2015; Adachi et al., 2016;
463 Landeen et al., 2016; Lesch et al., 2016; Zhang and Reed, 2016). Our approach for the
464 comparison of CREs across species, based on the analysis of differential histone
465 modification state in orthologous regions, demonstrated that cis-regulatory divergence
466 across species may be overestimated when based on the peak overlap status as a binary
467 variable.
468

469 **Specific genomic features are associated with CRE conservation**

470 Evolutionarily conserved promoters and enhancers have conserved nucleotide sequence,
471 are close to protein coding genes, are functional in many cell types, and harbor many
472 TFBSs. Many regulatory pathways, specifically those involved in the regulation of liver
473 function and housekeeping functions, are strongly conserved across primates, while other
474 pathways, such as immune response, are less constrained and evolve more rapidly. This

475 observation is consistent with the expected arms-race in evolution between host and
476 pathogens.
477
478 **Newly evolved CREs are derived from TE exaptation**
479 Based on our findings, exaptation of transposable elements into functional promoters and
480 enhancers is a pervasive phenomenon in primate genomes. LTRs and SVAs are the most
481 frequently exapted in humans and other apes, despite not being among the most common
482 transposable elements in the genome. Primate liver CREs are enriched in young TEs.
483 These young TEs, after being recruited into the primate regulatory network, introduced
484 novel gene expression in the associated species. To our knowledge, this is the first study
485 demonstrating how specific genomic features are associated to the recruitment of TEs as
486 functional elements in the primate regulatory landscape. In contrast, only a minor fraction of
487 the evolutionarily conserved CREs overlap an annotated TE. This suggests the action of
488 strong selection against the disruption of these regulatory elements, in order to maintain
489 stable gene expression. Further, these data suggest that the core regulatory network that
490 establishes liver cell-type identity is very conserved, whereas adaptive evolution occurs on
491 the periphery of the network, where TEs have the most impact on gene regulatory
492 evolution.
493
494 **Data availability**
495 All non-human raw sequence data have been deposited in the Sequence Read Archive
496 under following BioProject IDs: PRJNA349047 for RNA-seq and PRJNA349046 for ChIP-
497 seq data.
498
499 **Supplemental information**
500 Supplemental can be found with this article online at **xxxxxxxx**
501
502 **Author contributions**
503 MT, MC and CDB conceived the project. MT, YP, GHP and CDB designed the taxon
504 sampling and experiments. MT performed ChIP-seq and RNA-seq experiments. MT and
505 MHB performed the parallelized reporter assays. MHB and KA produced luciferase assay
506 data on *GRIN3A* and *JARID2*. KM and VJL designed and performed the luciferase assays
507 on the 69 TE families. MT, VJL and KM performed the TE enrichment analysis. YP
508 designed computational pipelines for the detection of orthologous regions in the Ensembl

MSA alignment and all related analyses. MT, YP and CDB analyzed the data and wrote the paper. All authors read and approved the manuscript.

Acknowledgements

We thank Texas Biomedical Research Institute, Duke University Lemur Center and the Hospital of University of Pennsylvania for providing the samples. We thank Jonathan Schug and other members of UPenn NGS Core Facility. We are grateful to Sarah Tishkoff, Yoseph Barash, Benjamin Voight, Yana Kamberov, Erin Fry, and Barbara Engelhardt for providing insightful comments on the preliminary versions of the results and of the manuscript.

519 **References**

520

521 Adachi, N., Robinson, M., Goolsbee, A., and Shubin, N.H. (2016). Regulatory evolution of
522 Tbx5 and the origin of paired appendages. Proceedings of the National Academy of
523 Sciences.

524 Andersson, R., Gebhard, C., Miguel-Escalada, I., Hoof, I., Bornholdt, J., Boyd, M., Chen, Y.,
525 Zhao, X., Schmidl, C., Suzuki, T., et al. (2014). An atlas of active enhancers across human
526 cell types and tissues. Nature *507*, 455–461.

527 Austenaa, L.M.I., Barozzi, I., Simonatto, M., Masella, S., Della Chiara, G., Ghisletti, S.,
528 Curina, A., de Wit, E., Bouwman, B.A.M., de Pretis, S., et al. Transcription of Mammalian
529 cis-Regulatory Elements Is Restrained by Actively Enforced Early Termination. Molecular
530 Cell *60*, 460–474.

531 Babbitt, C.C., Fedrigo, O., Pfefferle, A.D., Boyle, A.P., Horvath, J.E., Furey, T.S., and Wray,
532 G.A. (2010). Both Noncoding and Protein-Coding RNAs Contribute to Gene Expression
533 Evolution in the Primate Brain. Genome Biology and Evolution *2*, 67–79.

534 Bailey, T.L. (2011). DREME: motif discovery in transcription factor ChIP-seq data.
535 Bioinformatics *27*, 1653–1659.

536 Bailey, T.L., Boden, M., Buske, F.A., Frith, M., Grant, C.E., Clementi, L., Ren, J., Li, W.W.,
537 and Noble, W.S. (2009). MEME SUITE: tools for motif discovery and searching. Nucleic
538 Acids Res *37*, W202-208.

539 Ballester, B., Medina-Rivera, A., Schmidt, D., Gonzàlez-Porta, M., Carlucci, M., Chen, X.,
540 Chessman, K., Faure, A.J., Funnell, A.P., Goncalves, A., et al. (2014). Multi-species, multi-
541 transcription factor binding highlights conserved control of tissue-specific biological
542 pathways. eLife *3*, e02626.

543 Barnabas, S., Hai, T., and Andrisani, O.M. (1997). The Hepatitis B Virus X Protein
544 Enhances the DNA Binding Potential and Transcription Efficacy of bZip Transcription
545 Factors. Journal of Biological Chemistry *272*, 20684–20690.

546 Bejerano, G., Lowe, C.B., Ahituv, N., King, B., Siepel, A., Salama, S.R., Rubin, E.M., James
547 Kent, W., and Haussler, D. (2006). A distal enhancer and an ultraconserved exon are
548 derived from a novel retroposon. Nature *441*, 87–90.

549 Bourque, G., Leong, B., Vega, V.B., Chen, X., Lee, Y.L., Srinivasan, K.G., Chew, J.-L.,
550 Ruan, Y., Wei, C.-L., Ng, H.H., et al. (2008). Evolution of the mammalian transcription factor
551 binding repertoire via transposable elements. Genome Research.

552 Boyd, J.L., Skove, S.L., Rouanet, J.P., Pilaz, L.-J., Bepler, T., Gordân, R., Wray, G.A., and
553 Silver, D.L. Human-Chimpanzee Differences in a FZD8 Enhancer Alter Cell-Cycle
554 Dynamics in the Developing Neocortex. Current Biology *25*, 772–779.

555 Boyle, A.P., Araya, C.L., Brdlik, C., Cayting, P., Cheng, C., Cheng, Y., Gardner, K., Hillier,
556 L.W., Janette, J., Jiang, L., et al. (2014). Comparative analysis of regulatory information and
557 circuits across distant species. Nature *512*, 453–456.

558 Brawand, D., Soumillon, M., Necsulea, A., Julien, P., Csardi, G., Harrigan, P., Weier, M.,
559 Liechti, A., Aximu-Petri, A., Kircher, M., et al. (2011). The evolution of gene expression
560 levels in mammalian organs. Nature *478*, 343–348.

561 Breschi, A., Djebali, S., Gillis, J., Pervouchine, D.D., Dobin, A., Davis, C.A., Gingeras, T.R.,
562 and Guigó, R. (2016). Gene-specific patterns of expression variation across organs and
563 species. Genome Biology *17*, 1–13.

564 Britten, R.J., and Davidson, E.H. (1969). Gene Regulation for Higher Cells: A Theory.
565 Science *165*, 349–357.

566 Brosius, J., Gould, S.J. (1992). On “genomenclature": a comprehensive (and respectful)
567 taxonomy for pseudogenes and other “junk DNA.”. Proceedings of the National Academy of
568 Sciences USA *89*, 10706–10710.

569 Brown, C.D., Johnson, D.S., and Sidow, A. (2007). Functional Architecture and Evolution of
570 Transcriptional Elements That Drive Gene Coexpression. Science *317*, 1557.

571 Cain, C.E., Blekhman, R., Marioni, J.C., and Gilad, Y. (2011). Gene Expression Differences
572 Among Primates Are Associated With Changes in a Histone Epigenetic Modification.
573 Genetics *187*, 1225–1234.

574 Chuong, E.B., Rumi, M.A.K., Soares, M.J., and Baker, J.C. (2013). Endogenous
575 retroviruses function as species-specific enhancer elements in the placenta. Nat Genet *45*,
576 325–329.

577 Chuong, E.B., Elde, N.C., and Feschotte, C. (2016). Regulatory evolution of innate
578 immunity through co-option of endogenous retroviruses. Science *351*, 1083–1087.

579 Cohen, C.J., Lock, W.M., and Mager, D.L. (2009). Endogenous retroviral LTRs as
580 promoters for human genes: A critical assessment. Gene *448*, 105–114.

581 Coolon, J.D., McManus, C.J., Stevenson, K.R., Graveley, B.R., and Wittkopp, P.J. (2014).
582 Tempo and mode of regulatory evolution in Drosophila. Genome Research.

583 Cooper, G.M., and Brown, C.D. (2008). Qualifying the relationship between sequence
584 conservation and molecular function. Genome Research *18*, 201–205.

585 Core, L.J., Martins, A.L., Danko, C.G., Waters, C.T., Siepel, A., and Lis, J.T. (2014).
586 Analysis of nascent RNA identifies a unified architecture of initiation regions at mammalian
587 promoters and enhancers. Nat Genet *46*, 1311–1320.

588 Cotney, J., Leng, J., Yin, J., Reilly, S.K., DeMare, L.E., Emera, D., Ayoub, A.E., Rakic, P.,
589 and Noonan, J.P. The Evolution of Lineage-Specific Regulatory Activities in the Human
590 Embryonic Limb. Cell *154*, 185–196.

591 Creyghton, M.P., Cheng, A.W., Welstead, G.G., Kooistra, T., Carey, B.W., Steine, E.J.,
592 Hanna, J., Lodato, M.A., Frampton, G.M., Sharp, P.A., et al. (2010). Histone H3K27ac
593 separates active from poised enhancers and predicts developmental state. Proceedings of
594 the National Academy of Sciences *107*, 21931–21936.

595 Cusanovich, D.A., Pavlovic, B., Pritchard, J.K., and Gilad, Y. (2014). The Functional
596 Consequences of Variation in Transcription Factor Binding. PLoS Genet *10*, e1004226.

597 Davidson, E., and Britten, R. (1979). Regulation of gene expression: possible role of
598 repetitive sequences. Science *204*, 1052–1059.

599 Degner, J.F., Pai, A.A., Pique-Regi, R., Veyrieras, J.B., Gaffney, D.J., et al. (2012). DNaseI
600 sensitivity QTLs are a major determinant of human expression variation. Nature, *482*, 390–
601 394.

602 DeLaForest, A., Nagaoka, M., Si-Tayeb, K., Noto, F.K., Konopka, G., Battle, M.A., and
603 Duncan, S.A. (2011). HNF4A is essential for specification of hepatic progenitors from
604 human pluripotent stem cells. Development *138*, 4143.

605 De Souza, F.S.J., Franchini, L.F., and Rubinstein, M. (2013). Exaptation of Transposable
606 Elements into Novel Cis-Regulatory Elements: Is the Evidence Always Strong? Molecular
607 Biology and Evolution *30*(6), 1239-1251.

608 Dong, X., Wang, X., Zhang, F., and Tian, W. (2016). Genome-Wide Identification of
609 Regulatory Sequences Undergoing Accelerated Evolution in the Human Genome. Mol Biol
610 Evol *33*, 2565–2575.

611 Du, J., Leung, A., Trac, C., Lee, M., Parks, B.W., Lusis, A.J., Natarajan, R., and Schones,
612 D.E. (2016). Chromatin variation associated with liver metabolism is mediated by
613 transposable elements. Epigenetics Chromatin *9*, 28.

614 Eden, E., Lipson, D., Yogev, S., and Yakhini, Z. (2007). Discovering Motifs in Ranked Lists
615 of DNA Sequences. PLoS Comput Biol *3*, e39.

616 Eden, E., Navon, R., Steinfeld, I., Lipson, D., and Yakhini, Z. (2009). GOrilla: a tool for
617 discovery and visualization of enriched GO terms in ranked gene lists. BMC Bioinformatics
618 *10*, 1–7.

619 Emera, D., Yin, J., Reilly, S.K., Gockley, J., and Noonan, J.P. (2016). Origin and evolution
620 of developmental enhancers in the mammalian neocortex. Proceedings of the National
621 Academy of Sciences *113*, E2617–E2626.

622 ENCODE Project Consortium (2012). An integrated encyclopedia of DNA elements in the
623 human genome. Nature *489*, 57–74.

624 Fazio, G., Palmi, C., Rolink, A., Biondi, A., Cazzaniga, G. (2008). PAX5/TEL acts as a
625 transcriptional repressor causing down-modulation of CD19, enhances migration to
626 CXCL12, and confers survival advantage in pre-BI cells. Cancer Research *68*(1), 181–189.

627 FANTOM Consortium and the RIKEN PMI and CLST (DGT) (2014). A promoter-level
628 mammalian expression atlas. Nature *507*, 462–470.

629 Gittelman, R.M., Hun, E., Ay, F., Madeoy, J., Pennacchio, L., Noble, W.S., Hawkins, R.D.,
630 and Akey, J.M. (2015). Comprehensive identification and analysis of human accelerated
631 regulatory DNA. Genome Res *25*, 1245–1255.

632 Gross, L. (2005). Selection on a Neural Gene Regulator Sheds Light on Human Evolution.
633 PLoS Biol *3*, e417.

634 Grueber, C.E., Wallis, G.P., and Jamieson, I.G. (2014). Episodic Positive Selection in the
635 Evolution of Avian Toll-Like Receptor Innate Immunity Genes. PLoS ONE *9*, e89632.

636 Guo, C., Ludvik, A.E., Arlotto, M.E., Hayes, M.G., Armstrong, L.L., Scholtens, D.M., Brown,
637 C.D., Newgard, C.B., Becker, T.C., Layden, B.T., et al. (2015). Coordinated regulatory

638 variation associated with gestational hyperglycaemia regulates expression of the novel
639 hexokinase HKDC1. Nat Commun *6*.

640 Hah, N., Murakami, S., Nagari, A., Danko, C.G., and Kraus, W.L. (2013). Enhancer
641 transcripts mark active estrogen receptor binding sites. Genome Research *23*, 1210–1223.

642 Hancks, D.C., and Kazazian Jr., H.H. (2010). SVA retrotransposons: Evolution and genetic
643 instability. Seminars in Cancer Biology *20*, 234–245.

644 Ho, M.C.W., Johnsen, H., Goetz, S.E., Schiller, B.J., Bae, E., Tran, D.A., Shur, A.S., Allen,
645 J.M., Rau, C., Bender, W., et al. (2009). Functional Evolution of cis-Regulatory Modules at
646 a Homeotic Gene in Drosophila. PLoS Genet *5*, e1000709.

647 Holloway, A.K., Bruneau, B.G., Sukonnik, T., Rubenstein, J.L., and Pollard, K.S. (2016).
648 Accelerated Evolution of Enhancer Hotspots in the Mammal Ancestor. Molecular Biology
649 and Evolution *33*, 1008–1018.

650 Innocenti, F., Cooper, G.M., Stanaway, I.B., Gamazon, E.R., Smith, J.D., Mirkov, S.,
651 Ramirez, J., Liu, W., Lin, Y.S., Moloney, C., et al. (2011). Identification, Replication, and
652 Functional Fine-Mapping of Expression Quantitative Trait Loci in Primary Human Liver
653 Tissue. PLoS Genet *7*, e1002078.

654 Jain, D., Baldi, S., Zabel, A., Straub, T., and Becker, P.B. (2015). Active promoters give rise
655 to false positive “Phantom Peaks” in ChIP-seq experiments. Nucleic Acids Res *43*, 6959–
656 6968.

657 Jansa, A.S., Lundrigan, L.B., and Tucker, K.P. (2003). Tests for Positive Selection on
658 Immune and Reproductive Genes in Closely Related Species of the Murine Genus Mus.
659 Journal of Molecular Evolution *56*, 294–307.

660 Jordan, I.K., Rogozin, I.B., Glazko, G.V., and Koonin, E.V. (2003). Origin of a substantial
661 fraction of human regulatory sequences from transposable elements. Trends in Genetics
662 *19*, 68–72.

663 Kaneko, S., Bonasio, R., Saldaña-Meyer, R., Yoshida, T., Son, J., Nishino, K., Umezawa,
664 A., and Reinberg, D. Interactions between JARID2 and Noncoding RNAs Regulate PRC2
665 Recruitment to Chromatin. Molecular Cell *53*, 290–300.

666 Kapusta, A., Kronenberg, Z., Lynch, V.J., Zhuo, X., Ramsay, L., Bourque, G., Yandell, M.,
667 and Feschotte, C. (2013). Transposable Elements Are Major Contributors to the Origin,

668 Diversification, and Regulation of Vertebrate Long Noncoding RNAs. PLoS Genet *9*,
669 e1003470.

670 King, M., and Wilson, A. (1975). Evolution at two levels in humans and chimpanzees.
671 Science *188*, 107–116.

672 Kunarso, G., Chia, N.-Y., Jeyakani, J., Hwang, C., Lu, X., Chan, Y.-S., Ng, H.-H., and
673 Bourque, G. (2010). Transposable elements have rewired the core regulatory network of
674 human embryonic stem cells. Nat Genet *42*, 631–634.

675 Landeen, E.L., Muirhead, C.A., Wright, L., Meiklejohn, C.D., and Presgraves, D.C. (2016).
676 Sex Chromosome-wide Transcriptional Suppression and Compensatory Cis-Regulatory
677 Evolution Mediate Gene Expression in the Drosophila Male Germline. PLoS Biol *14*,
678 e1002499.

679 Lazzaro, B.P., and Schneider, D.S. (2014). The Genetics of Immunity. G3:
680 Genes|Genomes|Genetics *4*, 943–945.

681 Lecomte, V., Maugnier, E., Euthine, V., Durand, C., Freyssenet, D., Nemoz, G., Rome, S.,
682 Vidal, H. and Lefai, E. (2010). A new role for sterol regulatory element binding protein 1
683 transcription factors in the regulation of muscle mass and muscle cell differentiation.
684 Molecular and Cell Biology *30*(5), 1182–1189.

685 Lesch, B.J., Silber, S.J., McCarrey, J.R., and Page, D.C. (2016). Parallel evolution of male
686 germline epigenetic poising and somatic development in animals. Nat Genet *48*, 888–894.

687 Lewis, J.J., van der Burg, K.R.L., Mazo-Vargas, A., and Reed, R.D. ChIP-Seq-Annotated
688 Heliconius erato Genome Highlights Patterns of cis-Regulatory Evolution in Lepidoptera.
689 Cell Reports *16*, 2855–2863.

690 Li, H. (2013) Aligning sequence reads, clone sequences and assembly contigs with BWA-
691 MEM. arXiv:1303.3997v1

692 Li, W., Notani, D., and Rosenfeld, M.G. (2016). Enhancers as non-coding RNA transcription
693 units: recent insights and future perspectives. Nat Rev Genet *17*, 207–223.

694 Liao, Y., Smyth, G.K., and Shi, W. (2014). featureCounts: an efficient general purpose
695 program for assigning sequence reads to genomic features. Bioinformatics *30*, 923–930.

696 Loisel, D.A., Rockman, M.V., Wray, G.A., Altmann, J., and Alberts, S.C. (2006). Ancient
697 polymorphism and functional variation in the primate MHC-DQA1 5′ cis-regulatory region.
698 Proceedings of the National Academy of Sciences *103*, 16331–16336.

699 Love, M.I., Huber, W., and Anders, S. (2014). Moderated estimation of fold change and
700 dispersion for RNA-seq data with DESeq2. Genome Biology *15*, 1–21.

701 Lynch, V.J., Leclerc, R.D., May, G., and Wagner, G.P. (2011). Transposon-mediated
702 rewiring of gene regulatory networks contributed to the evolution of pregnancy in mammals.
703 Nat Genet *43*, 1154–1159.

704 Lynch, V.J., Nnamani, M.C., Kapusta, A., Brayer, K., Plaza, S.L., Mazur, E.C., Emera, D.,
705 Sheikh, S.Z., Grützner, F., Bauersachs, S., et al. (2015) Ancient Transposable Elements
706 Transformed the Uterine Regulatory Landscape and Transcriptome during the Evolution of
707 Mammalian Pregnancy. Cell Reports *10*, 551–561.

708 Markljung, E., Jiang, L., Jaffe, J.D., Mikkelsen, T.S., Wallerman, O., Larhammar, M., Zhang,
709 X., Wang, L., Saenz-Vash, V., Gnirke, A., et al. (2009). ZBED6, a Novel Transcription
710 Factor Derived from a Domesticated DNA Transposon Regulates IGF2 Expression and
711 Muscle Growth. PLoS Biol *7*, e1000256.

712 Marnetto, D., Molineris, I., Grassi, E., and Provero, P. (2014). Genome-wide Identification
713 and Characterization of Fixed Human-Specific Regulatory Regions. American Journal of
714 Human Genetics *95*, 39–48.

715 Martin, A., and Reed, R.D. (2014). Wnt signaling underlies evolution and development of
716 the butterfly wing pattern symmetry systems. Developmental Biology *395*, 367–378.

717 Martin, A., Papa, R., Nadeau, N.J., Hill, R.I., Counterman, B.A., Halder, G., Jiggins, C.D.,
718 Kronforst, M.R., Long, A.D., McMillan, W.O., et al. (2012). Diversification of complex
719 butterfly wing patterns by repeated regulatory evolution of a Wnt ligand. Proceedings of the
720 National Academy of Sciences *109*, 12632–12637.

721 Maurano, M.T., Humbert, R., Rynes, E., Thurman, R.E., Haugen, E., et al. (2012).
722 Systematic Localization of Common Disease-Associated Variation in Regulatory DNA.
723 Science, *337*, 1190–1195.

724 Maurer, P., Tsas, F., Coutte, L., Callens, N., Brenner, C., Van Lint, C., de Launoit, Y., Baert,
725 JL (2003). FEV acts as a transcriptional repressor through its DNA-binding ETS domain
726 and alanine-rich domain. Oncogene *22*(21), 3319–3329.

727 McClintock, B. (1950). The Origin and Behavior of Mutable Loci in Maize. Proceedings of
728 the National Academy of Sciences of the United States of America *36*, 344–355.

729 McClintock, B. (1984). The significance of responses of the genome to challenge. Science
730 *226*, 792–801.

731 Melnikov, A., Murugan, A., Zhang, X., Tesileanu, T., Wang, L., Rogov, P., Feizi, S., Gnirke,
732 A., Callan, C.G., Kinney, J.B., et al. (2012). Systematic dissection and optimization of
733 inducible enhancers in human cells using a massively parallel reporter assay. Nat Biotech
734 *30*, 271–277.

735 Musunuru, K., Strong, A., Frank-Kamenetsky, M., Lee, N.E., Ahfeldt, T., Sachs, K.V., Li, X.,
736 Li, H., Kuperwasser, N., Ruda, V.M., et al. (2010). From noncoding variant to phenotype via
737 SORT1 at the 1p13 cholesterol locus. Nature, *466* (7307), 714–719.

738 Patwardhan, R.P., Hiatt, J.B., Witten, D.M., Kim, M.J., Smith, R.P., May, D., Lee, C.,
739 Andrie, J.M., Lee, S.-I., Cooper, G.M., et al. (2012). Massively parallel functional dissection
740 of mammalian enhancers in vivo. Nat Biotech *30*, 265–270.

741 Obbard, D.J., Welch, J.J., Kim, K.-W., and Jiggins, F.M. (2009). Quantifying Adaptive
742 Evolution in the Drosophila Immune System. PLoS Genet *5*, e1000698.

743 Ori, A., Atzmony, D., Haviv, I., and Shaul, Y. (1994). An NF1 Motif Plays a Central Role in
744 Hepatitis B Virus Enhancer. Virology *204*, 600–608.

745 Perelman, P., Johnson, W.E., Roos, C., Seuánez, H.N., Horvath, J.E., Moreira, M.A.M.,
746 Kessing, B., Pontius, J., Roelke, M., Rumpler, Y., et al. (2011). A Molecular Phylogeny of
747 Living Primates. PLoS Genet *7*, e1001342.

748 Pickrell, J.K., Gaffney, D.J., Gilad, Y., and Pritchard, J.K. (2011). False positive peaks in
749 ChIP-seq and other sequencing-based functional assays caused by unannotated high copy
750 number regions. Bioinformatics *27*, 2144–2146.

751 Pollard, K.S., Salama, S.R., King, B., Kern, A.D., Dreszer, T., Katzman, S., Siepel, A.,
752 Pedersen, J.S., Bejerano, G., Baertsch, R., et al. (2006). Forces Shaping the Fastest
753 Evolving Regions in the Human Genome. PLoS Genet *2*, e168.

754 Pollard, K.S., Hubisz, M.J., Rosenbloom, K.R., and Siepel, A. (2010). Detection of
755 nonneutral substitution rates on mammalian phylogenies. Genome Research *20*, 110–121.

756 Prabhakar, S., Visel, A., Akiyama, J.A., Shoukry, M., Lewis, K.D., Holt, A., Plajzer-Frick, I.,
757 Morrison, H., FitzPatrick, D.R., Afzal, V., et al. (2008). Human-Specific Gain of Function in a
758 Developmental Enhancer. Science *321*, 1346–1350.

759 Prescott, S.L., Srinivasan, R., Marchetto, M.C., Grishina, I., Narvaiza, I., Selleri, L., Gage,
760 F.H., Swigut, T., and Wysocka, J. Enhancer Divergence and cis-Regulatory Evolution in the
761 Human and chimpanzee Neural Crest. Cell *163*, 68–83.

762 Rayan, N.A., Del Rosario, R.C.H., and Prabhakar, S. (2016). Massive contribution of
763 transposable elements to mammalian regulatory sequences. Semin Cell Dev Biol *57*, 51–
764 56.

765 Reilly, S.K., Yin, J., Ayoub, A.E., Emera, D., Leng, J., Cotney, J., Sarro, R., Rakic, P., and
766 Noonan, J.P. (2015). Evolutionary changes in promoter and enhancer activity during human
767 corticogenesis. Science *347*, 1155–1159.

768 del Rosario, R.C.H., Rayan, N.A., and Prabhakar, S. (2014). Noncoding origins of
769 anthropoid traits and a new null model of transposon functionalization. Genome Research
770 *24*, 1469–1484.

771 Sackton, T.B., Lazzaro, B.P., Schlenke, T.A., Evans, J.D., Hultmark, D., and Clark, A.G.
772 (2007). Dynamic evolution of the innate immune system in Drosophila. Nat Genet *39*,
773 1461–1468.

774 Salazar-Jaramillo, L., Paspati, A., van de Zande, L., Vermeulen, C.J., Schwander, T., and
775 Wertheim, B. (2014). Evolution of a cellular immune response in Drosophila: a phenotypic
776 and genomic comparative analysis. Genome Biol Evol *6*, 273–289.

777 Sasaki, T., Nishihara, H., Hirakawa, M., Fujimura, K., Tanaka, M., Kokubo, N., Kimura-
778 Yoshida, C., Matsuo, I., Sumiyama, K., Saitou, N., et al. (2008). Possible involvement of
779 SINEs in mammalian-specific brain formation. Proceedings of the National Academy of
780 Sciences *105*, 4220–4225.

781 Schadt, E.E. (2009). Molecular networks as sensors and drivers of common human
782 diseases. Nature *461*, 218–223.

783 Schmidt, D., Wilson, M.D., Ballester, B., Schwalie, P.C., Brown, G.D., Marshall, A., Kutter,
784 C., Watt, S., Martinez-Jimenez, C.P., Mackay, S., et al. (2010). Five-Vertebrate ChIP-seq
785 Reveals the Evolutionary Dynamics of Transcription Factor Binding. Science *328*, 1036.

786 Schmidt, D., Schwalie, P.C., Wilson, M.D., Ballester, B., Gonçalves, Â., Kutter, C., Brown,
787 G.D., Marshall, A., Flicek, P., and Odom, D.T. (2012). Waves of Retrotransposon
788 Expansion Remodel Genome Organization and CTCF Binding in Multiple Mammalian
789 Lineages. Cell *148*, 335–348.

790 Sharon, E., Kalma, Y., Sharp, A., Raveh-Sadka, T., Levo, M., Zeevi, D., Keren, L., Yakhini,
791 Z., Weinberger, A., and Segal, E. (2012). Inferring gene regulatory logic from high-
792 throughput measurements of thousands of systematically designed promoters. Nat Biotech
793 *30*, 521–530.

794 Siepel, A., Bejerano, G., Pedersen, J.S., Hinrichs, A.S., Hou, M., Rosenbloom, K., Clawson,
795 H., Spieth, J., Hillier, L.W., Richards, S., et al. (2005). Evolutionarily conserved elements in
796 vertebrate, insect, worm, and yeast genomes. Genome Research *15*, 1034–1050.

797 Sironi, M., Cagliani, R., Forni, D., and Clerici, M. (2015). Evolutionary insights into host-
798 pathogen interactions from mammalian sequence data. Nat Rev Genet *16*, 224–236.

799 Smedley, D., Haider, S., Durinck, S., Pandini, L., Provero, P., Allen, J., Arnaiz, O., Awedh,
800 M.H., Baldock, R., Barbiera, G., et al. (2015). The BioMart community portal: an innovative
801 alternative to large, centralized data repositories. Nucleic Acids Research *43*, W589–W598.

802 Sundaram, V., Cheng, Y., Ma, Z., Li, D., Xing, X., Edge, P., Snyder, M.P., and Wang, T.
803 (2014). Widespread contribution of transposable elements to the innovation of gene
804 regulatory networks. Genome Res *24*, 1963–1976.

805 Takata, A., Iwayama, Y., Fukuo, Y., Ikeda, M., Okochi, T., Maekawa, M., Toyota, T.,
806 Yamada, K., Hattori, E., Ohnishi, T., et al. A Population-Specific Uncommon Variant in
807 GRIN3A Associated with Schizophrenia. Biological Psychiatry *73*, 532–539.

808 Tsankov, A.M., Thompson, D.A., Socha, A., Regev, A., and Rando, O.J. (2010). The Role
809 of Nucleosome Positioning in the Evolution of Gene Regulation. PLoS Biol *8*, e1000414.

810 Vallender, E.J., and Lahn, B.T. (2004). Positive selection on the human genome. Human
811 Molecular Genetics *13*, R245–R254.

812 Villar, D., Berthelot, C., Aldridge, S., Rayner, T.F., Lukk, M., Pignatelli, M., Park, T.J.,
813 Deaville, R., Erichsen, J.T., Jasinska, A.J., et al. Enhancer Evolution across 20 Mammalian
814 Species. Cell *160*, 554–566.

815 Wallerman, O., Motallebipour, M., Enroth, A., Patra, K., Bysani, M.S.R., Komorowski, J.,
816 and Wadelius, C. (2009). Molecular interactions between HNF4a, FOXA2 and GABP
817 identified at regulatory DNA elements through ChIP-sequencing. Nucleid Acids Research
818 *37*, 7498–7508.

819 Wang, T., Zeng, J., Lowe, C.B., Sellers, R.G., Salama, S.R., Yang, M., Burgess, S.M.,
820 Brachmann, R.K., and Haussler, D. (2007). Species-specific endogenous retroviruses

821 shape the transcriptional network of the human tumor suppressor protein p53. Proceedings
822 of the National Academy of Sciences *104*, 18613–18618.

823 Warner, L.R., Babbitt, C.C., Primus, A.E., Severson, T.F., Haygood, R., and Wray, G.A.
824 (2009). Functional consequences of genetic variation in primates on tyrosine hydroxylase
825 (TH) expression in vitro. Brain Research *1288*, 1–8.

826 Wertheim, B. (2015). Genomic basis of evolutionary change: evolving immunity. Frontiers in
827 Genetics *6*, 222.

828 Wray, G.A. (2007). The evolutionary significance of cis-regulatory mutations. Nat Rev
829 Genet *8*, 206–216.

830 Xie, M., Hong, C., Zhang, B., Lowdon, R.F., Xing, X., Li, D., Zhou, X., Lee, H.J., Maire, C.L.,
831 Ligon, K.L., et al. (2013). DNA hypomethylation within specific transposable element
832 families associates with tissue-specific enhancer landscape. Nat Genet *45*, 836–841.

833 Yang, S., Oksenberg, N., Takayama, S., Heo, S.-J., Poliakov, A., Ahituv, N., Dubchak, I.,
834 and Boffelli, D. (2015). Functionally conserved enhancers with divergent sequences in
835 distant vertebrates. BMC Genomics *16*, 1–13.

836 Yates, A., Beal, K., Keenan, S., McLaren, W., Pignatelli, M., Ritchie, G.R.S., Ruffier, M.,
837 Taylor, K., Vullo, A., and Flicek, P. (2015). The Ensembl REST API: Ensembl Data for Any
838 Language. Bioinformatics *31*, 143–145.

839 Young, R.S., Kumar, Y., Bickmore, W.A., and Taylor, M.S. (2016). Bidirectional
840 transcription marks accessible chromatin and is not specific to enhancers. bioRxiv.

841 Zak, D.E., Tam, V.C., and Aderem, A. (2014). Systems-Level Analysis of Innate Immunity.
842 Annu. Rev. Immunol. *32*, 547–577.

843 Zhang, L., and Reed, R.D. (2016). Genome editing in butterflies reveals that spalt promotes
844 and Distal-less represses eyespot colour patterns. Nat Commun *7*.

845 Zhang, Y., Liu, T., Meyer, C.A., Eeckhoute, J., Johnson, D.S., Bernstein, B.E., Nusbaum,
846 C., Myers, R.M., Brown, M., Li, W., et al. (2008). Model-based Analysis of ChIP-Seq
847 (MACS). Genome Biology *9*, 1–9.

848 Zhou, X., Cain, C.E., Myrthil, M., Lewellen, N., Michelini, K., Davenport, E.R., Stephens, M.,
849 Pritchard, J.K., and Gilad, Y. (2014). Epigenetic modifications are associated with inter-
850 species gene expression variation in primates. Genome Biology *15*, 1–19.
851

852

853 ## Materials and Methods

854

855 **Tissue sampling**

856 We obtained liver tissue samples for three to four individuals belonging to each of the
857 studied primate species (three bushbabies, four chimpanzees, three humans, three
858 marmosets, three mouse lemurs, and three rhesus macaques; Table S1). Samples for
859 chimpanzees, marmoset and rhesus macaque were obtained from Texas Biomedical
860 Research Institute (San Antonio, TX); bushbaby and mouse lemur livers were obtained
861 from the Lemur Center of Duke University (Durham, NC). Tissue samples were collected
862 and flash-frozen immediately. With the exception of the bushbaby, samples for all of the
863 species included both males and females (Table S1). Age was comparable across species
864 (young adults) and all individuals died of causes unrelated to liver disease.

865

866 **RNA-seq sample processing**

867 We processed samples from all species in random batches of four in order to minimize
868 batch effects. For each sample, 25 mg of frozen liver tissue was used to extract total RNA
869 and genomic DNA, using QIAGEN AllPrep DNA/RNA/miRNA Universal Kit. Quality of total
870 RNA was assessed computing the RNA Integrity Number (RIN) using Agilent Bioanalyzer.
871 All RNA samples had a RIN > 8. We used 4µg aliquots of total RNA to produce barcoded
872 RNA sequencing libraries using the Illumina TruSeq Stranded mRNA kit. The quality of
873 generated libraries was assessed using Agilent Bioanalyzer High Sensitivity DNA Kit and
874 Kapa metrics. Libraries were pooled in two different pools based on barcode compatibility,
875 and each pool was sequenced in two Illumina HiSeq2500 lanes, producing on an average
876 of 42.1 million single end (SE) 100-bp reads per sample.

877

878 **ChIP-seq sample processing**

879 We processed samples in six randomly assigned groups in order to minimize batch effects.
880 For each sample, we cut 90 mg of frozen liver tissue into 1 mm^3 pieces, washed the cut
881 tissue samples with cold phosphate-buffered saline (PBS), and fixed with 1% formaldehyde
882 for 5 minutes at room temperature. We prepared nuclei of each washed sample using the
883 Covaris truChIP Tissue Chromatin Shearing Kit. Chromatin was then sheared for 16
884 minutes using a Covaris S220 Focused-ultrasonicator. We quantified shearing efficiency
885 and chromatin concentration using Agilent Bioanalyzer High Sensitivity DNA Kit.

886 From each specimen, we kept aside a 0.5 µg aliquot of sheared chromatin to be
887 used as input. We used two 5 µg aliquots of chromatin per sample to perform
888 immunoprecipitation (IP) with antibodies directed at H3K27ac (ab4729) and H3K4me1
889 (ab8895) respectively. We performed each IP using 5 µg of antibody with an overnight
890 incubation at 4°C as specified by the Magna ChIP A/G Chromatin Immunoprecipitation Kit
891 protocol. After elution and protein-DNA crosslink reversal, we extracted DNA using Zymo
892 Research ChIP DNA Clean & Concentrator kit, and quantified extracted DNA using Agilent
893 High Sensitivity kit and Qubit 2.0.
894 We used 5 to 15 ng of input and immunoprecipitated DNA to generate sequencing
895 libraries using the NEBNext Ultra ChIPseq library kit, following protocols specified by the
896 manufacturer. We assessed the quality of each constructed library using Agilent
897 Bioanalyzer High Sensitivity DNA Kit and Kapa metrics. Libraries were multiplexed, pooled
898 and sequenced on a total of 16 Illumina HiSeq2500 lanes, producing on an average of 40.6
899 million SE 100-bp reads per sample.
900
901 **Sequence QC: ChIP-seq and RNA-seq**
902 We performed the standard quality control (QC) measures on both ChIP-seq and RNA-seq
903 fastq files using FastQC v0.11.3 (Andrews, 2010). We then trimmed sequencing adapters
904 and low quality base calls using TrimGalore! v0.4.1 with the following parameters: -
905 stringency 5 -length 50 -q 20
906 (http://www.bioinformatics.babraham.ac.uk/projects/trim_galore/).
907
908 **RNA-seq alignment and gene expression quantification**
909 We aligned all sequences that passed QC to the reference genomes from the Ensembl
910 database (bushbaby: otoGar3; chimp: CHIMP2.1.4; humans: GRCh38; rhesus macaque:
911 Mmul1; marmoset: C_jacchus3.2.1; mouse lemur: micMur1) using STAR v2.5 (Dobin et al.,
912 2013) in 2-pass mode with the following parameters: --quantMode TranscriptomeSAM --
913 outFilterMultimapNmax 10 --outFilterMismatchNmax 10 --outFilterMismatchNoverLmax 0.3
914 --alignIntronMin 21 --alignIntronMax 0 --alignMatesGapMax 0 --alignSJoverhangMin 5 --
915 runThreadN 12 --twopassMode Basic --twopass1readsN 60000000 --sjdbOverhang 100.
916 We filtered bam files based on alignment quality (q = 10) and sorted using Samtools
917 v0.1.19 sort function (Li, 2009). We used the latest annotations for each species obtained
918 from Ensembl to build reference indexes for the STAR alignment:
919 Homo_sapiens.GRCh38.82.chr.gtf; Pan_troglodytes.CHIMP2.1.4.82.chr.gtf;

920 Macaca_mulatta.MMUL_1.82.chr.gtf; Callithrix_jacchus.C_jacchus3.2.1.82.chr.gtf;
921 Otolemur_garnettii.OtoGar3.82.gtf; Microcebus_murinus.micMur1.82.gtf (Aken et al., 2016).
922 We used FeatureCounts (Liao et al., 2014) to count reads mapping to each protein coding
923 gene/lincRNA/pseudogene, according to Ensembl annotations for the six studied species.
924 Read counts were then normalized based on feature (gene) length.
925
926 **Differential gene expression analysis**
927 We analyzed differential gene expression levels for each species using read counts,
928 normalized by feature length with the DESeq2 software (Love et al., 2014), and with the
929 following model:
930 *design = ~condition*
931
932 where condition indicates the species or the group of species (e.g. apes).
933 We used a set of 10,243 genes annotated as orthologs in the six species according
934 to Ensembl (BioMart v. 0.9; Smedley et al., 2015; Table S3) and used 5% False Discovery
935 Rate (FDR) as our multiple-testing-corrected significance threshold. The overall analysis
936 included three main comparisons of our interest: 1) pairwise comparisons between human
937 and each of the other five species; 2) comparisons for human-specific differential
938 expression of orthologous genes (human versus other five primates grouped together); 3)
939 comparisons for ape-specific differential expression of orthologous genes (human +
940 chimpanzee versus other four primates).
941 4) comparisons for Catarrhini-specific differential expression (human+chimpanzee+rhesus
942 macaque versus other primates). Finally comparison between Strepsirrhini (human,
943 chimpanzee, rhesus macaque and marmoset) and Haplorrhini (mouse lemur and
944 bushbaby) was computed.
945
946 **ChIP-seq QC and alignment**
947 We applied standard QC measures to ChIP-seq data as described above for RNA-seq data
948 processing. We aligned the sequences that passed QC to the reference genomes from the
949 Ensembl database (bushbaby: otoGar3; chimpanzee: CHIMP2.1.4; humans: GRCh38;
950 rhesus macaque: Mmul1; marmoset: C_jacchus3.2.1; mouse lemur: micMur1) using
951 Burrows Wheeler Alignment tool (BWA), with the MEM algorithm (Li, 2013). We sorted the
952 filtered bam files using Samtools v0.1.19 (Li, 2009).
953

954 **ChIP-seq peak calling and QC**

955 We called peaks for each individual using MACS2 (Zhang et al., 2008), at 1% FDR, and
956 with parameters recommended for histone modifications (Liu, 2014): --m 30 40 --ext size
957 147 -B. Input was used as a control in all differential histone modification analyses. We
958 performed QC on peaks called for each specimen using metrics recommended by
959 ENCODE (Landt et al., 2012): Fraction of Reads in Peaks (FRiP), Normalize Strand
960 Correlation coefficient (NSC) and Relative Strand Correlation coefficient (RSC) and
961 ENCODE quality score.

962 In order to compute FRiP, we used Bedtools (v2.25.0; Quinlan and Hall, 2010) to
963 intersect bed files containing all coordinates of called peaks (narrowPeak output of MACS2)
964 with the original sorted bam file of the specific ChiP-seq sample. Then, we used a publicly
965 available perl script to count the reads mapping in the intersection
966 regions(https://github.com/mel-astar/mel-ngs/blob/master/mel-chipseq/chipseq-
967 metrics/getCnt.pl). As recommended by the ENCODE consortium, we selected a threshold
968 of 1% as acceptable FRiP values. We computed the two strand correlation metrics (NSC,
969 RSC) using Phantompeakqualtools (Landt et al., 2012). For H3K27ac, NSC ≥ 1.05 and
970 RSC ≥ 0.8 were used as threshold for retaining samples. For H3K4me1, that tends to
971 produce broader peaks, we used NSC ≥ 1.05 and RSC ≥ 0.5 (Table S1).

972 Samples that did not pass at least two of the three main QC metrics (FRiP, NSC,
973 RSC) were excluded for any downstream analysis. We then called human consensus
974 peaks for H3K27ac and H3K4me1 using MACS2 and the above described parameters with
975 the 1% FDR threshold. All human samples passing QC were considered as replicates of
976 each other for the consensus peak calling. These human consensus H3K27ac and
977 H3K4me1 profiles were used to perform all of the below described human-centric
978 downstream analyses. Peaks called for the other species were only used for the above
979 mentioned QC purposes but were not utilized for any of the downstream analyses, with the
980 exception of the chimpanzee consensus peaks (see below). In order to assess how our
981 data compares to known liver related regulatory regions, we overlapped our set of human
982 consensus peaks to the set of H3K27ac and H3K4me1 peaks generated for HepG2 cells
983 from the ENCODE consortium and to the set of permissive enhancers generated by the
984 FANTOM5 consortium.

985

986 **Comparison to previous findings using human liver ChIP-seq data**

987 We compared our human H3K27ac ChIP-seq data, with a set of published human liver
988 H3K27ac peaks (Villar et al., 2015). We used the window function of Bedtools to quantify
989 the number of H3K27ac peaks in the replication dataset that either overlap with, or are
990 found within 1 kb up- and downstream from each of our human H3K27ac peaks. With this
991 approach, we quantified and assessed overlaps between discovery and replication
992 datasets.

993 Next, we characterized sets of replicated and unreplicated peaks between the two
994 datasets. Using the procedures previously described for the comparison of conserved and
995 recently evolved CREs, we annotated several genomic features for both replicated and
996 unreplicated peaks. Specifically, we included information regarding: 1) the average distance
997 from the closest TSS; 2) the class of the associated gene (e.g., protein coding, lincRNA); 3)
998 the number of cell types with an overlapping ENCODE DHS site and; 4) the number of
999 ENCODE TFBS overlapping the peak. Moreover, a logistic regression on the q-values of
000 replicated and not replicated peaks was performed.

001

002 **Parallelized reporter assay**

003 We obtained a list of 334 putative 1-kb long CREs overlapping liver eQTLs from Brown and
004 collaborators (Brown et al., 2013). This data included both enhancers (distance from TSS >
005 1Kb) and promoters (distance from TSS < 1kb). 122 CREs out of these 334 CREs
006 overlapped our human ChIP-seq peaks (53 enhancers and 69 promoters; Table S6). Within
007 each of the loci defined by the investigated liver eQTLs, we predicted a 1-kb CRE. These
008 predicted CREs were amplified in individual PCRs performed on 120 pooled Yoruban
009 HapMap DNA samples. PCR products from each reaction therefore represent a complex
010 mixture of haplotypes. We inserted barcodes (hereafter, tags) consisting of a 160-bp oligo,
011 including a randomized 20-bp unique barcode for each construct, into luciferase reporter
012 vectors (pGL4.23 and pGL4.10), immediately downstream of the luciferase gene, after
013 linearizing the vector with the XbaI restriction enzyme.

014 We pooled and cloned DNAs from each putative CRE into uniquely barcoded
015 luciferase reporter vectors (pGL4.23 were used for enhancers and pGL4.10 for promoters),
016 using the Gibson Assembly Kit (New England BioLabs). The CREs were specifically
017 inserted upstream of the luciferase gene, after linearizing the vector with the restriction
018 enzymes KpnI and XhoI. We then transfected the complex pool of CRE reporters into
019 HepG2 cells in two replicates. 24 hours after transfection, we extracted total RNA, purified
020 poly-A RNA, and produced cDNA that was used to amplify the tag, with the QIAGEN One

021 Step RT-PCR Kit with primers that included Illumina adapters for sequencing. Tag libraries
022 were pooled and sequenced on a single Illumina HiSeq2500 lane, producing single end
023 (SE) 50-bp reads. We amplified the tags from the vector before the transfection and
024 sequenced them in the same pool with the tag-RNA libraries as a control for tag read
025 counts.

026 In parallel, reporter tags were unambiguously associated with each specific CRE by
027 sequence based sub-assembly. Briefly, we cut the luciferase gene from the vector by
028 inverse PCR and then re-ligated the vector using the T4 Polynucleotide Kinase (PNK) + T4
029 ligase kit from NEB. In this way CREs and tags were flanking each other and CRE-tag
030 complexes. The CRE-tag complexes were then PCR amplified using a reverse primer that
031 included Illumina adapter for sequencing. Next, the CRE-tag PCR product was digested for
032 5 minutes at 55°C using Nexetera Tn5 Transposase (TDE1) in order to produce fragments
033 of variable length (from ca. 150 bp to the entire length of the construct). When cutting the
034 fragments, TDE1 also inserts an Illumina compatible adapter in proximity of the cutting site.
035 We performed a PCR to enrich the libraries using the TDE1 inserted adapter as forward
036 primer and the previously included Illumina adapter as reverse primer.

037 We pooled the two libraries (one for pGL4.10 and one for pGL4.23 constructs) and
038 sequenced them on an Illumina MiSeq, producing paired-end (PE) reads (250 + 50 bp).
039 After performing QC with FastQC v0.11.3, we aligned the sub-assembly sequences to the
040 human genome (GRCh37/hg19) using BWA mem and the bam files were sorted and
041 indexed with Samtools v0.1.19. Finally, we produced a matrix listing all of the CRE-tag
042 associations. Tags associated with more than one CRE were discarded and not used for
043 further analyses. After attributing each tag to its uniquely associated CRE, we used
044 sequence based tag counts (HiSeq reads), normalized by sequencing depth, to quantify the
045 gene expression level driven by each CRE, and therefore its functionality as
046 enhancer/promoter.

047 For each CRE, we used a count-based generalized linear model to quantify
048 differential expression between RNA (after transfection) and DNA (before transfection),
049 assuming a Poisson error function:

050

051 *model= count~condition*

052

053 where condition indicates that the read count comes either from RNA (replicates 1 and 2) or
054 DNA-control.

In presence of a significant p-value, the model indicates a significant difference between the expression of the tags in the RNA samples compared to their DNA control. The effect size estimate was then used to infer whether the RNA samples were upregulated, hence showing significantly higher level of expression of the tags compared to their DNA controls, and therefore indicating that the CRE is a functional regulatory element.

Detection of orthologous regions for human peaks in each primate

We mapped orthologous sequences using all identified consensus ChIP-seq peak regions in both H3K27ac and H3K4me1 experiments. We used the Ensembl multiple sequence alignment (MSA) reference database with the following specifications: 39 Eutherian mammals; method_link_type: "EPO_LOW_COVERAGE"; species_set_name: "mammals" (Herrero et al., 2015). For orthologous sequence analysis, 500 bp up- and downstream regions were considered to be a part of the identified consensus peaks in all six species. We queried all regions directly from the reference database using the REST API (Yates et al., 2015).

All orthologous sequences retained gaps generated by MSA. In cases of incomplete chromosome assembly (e.g. mouse lemur), composite sequence representations containing parts of multiple scaffolds are used as a reference as provided by the Ensembl database. As a result, we independently queried each peak region as well as regions covering each peak +/- 500 bp. All orthologous sequences pulled from the references for downstream analysis contained only directly aligned sequences. All regions with no orthologous regions represented in the MSA reference were excluded from further analyses. All query results in .json format and extracted sequences formatted for the MSA alignment as well as genomic position information are provided in the repository mentioned in the final section.

Correlation between human and marmoset read counts within orthologous regions

We assessed human and marmoset (i.e. the species with the smallest number of peaks called; Supplemental File S1) normalized read counts at the 47,673 orthologous CREs, after splitting them into two groups: 1) regions with overlapping peaks present in both marmoset and human, and 2) regions with a peak present only in human. Spearman's correlation (ρ) between human and marmoset normalized read depths was then computed for each the two groups.

089 **Differential histone modification analysis**

090 Using the above described procedure, for both H3K27ac and H3K4me1, we produced a
091 single matrix including the human peaks having an ortholog in each of the studied species
092 and the associated read count for the specific histone mark and for the input in all of the six
093 species. The normalized read counts were used for differential ChIP-seq analysis with
094 DESeq2, performing an interaction analysis using the Wald statistic between the histone
095 marks read counts and their associated input values:

096

097 *design = ~assay + condition + assay:condition*

098

099 where the assay indicates either histone marks data or input data, and condition indicates
100 instead the species or the group of species (e.g. apes, Catarrhini, Haplorrhini).

101 Differential histone mark analysis included the same species × species and group ×
102 group comparisons described for RNA-seq. We used 10% FDR as our multiple testing
103 corrected significance threshold. Further, different FDRs (5%, 10%, 20%, 30%, 40%) were
104 tested to assess the robustness of our approach.

105 We analyzed differential histone modifications for the two marks independently.
106 However, in order to quantify the fraction of differentially marked cis-regulatory elements
107 (CREs) in all of the above described pairwise comparisons, we used bedtools to identify the
108 CREs predicted by H3K27ac (i.e. H3K27ac peaks) that would overlap those predicted by
109 H3K4me1 for at least a 25% of their length. The list of unique CREs was used to estimate
110 the fraction of differentially bound CREs for each of the above mentioned human-centric
111 pairwise comparisons. We defined CREs as evolutionarily conserved if they did not show
112 significant differential histone mark in any of the above mentioned pairwise comparisons.
113 Otherwise, the CRE were defined as recently evolved.

114

115 **Sequence conservation versus functional conservation analysis**

116 We estimated per-nucleotide pairwise divergence for all five species in comparison to
117 humans using MSA aligned sequences of orthologous regions for consensus peaks +/- 500
118 bps. All gaps in human were excluded from analysis. Regions not included in the set of six-
119 way orthologous CREs were also pruned. Finally, we removed outliers - with respect to the
120 distribution of the genetic distances in the given pairwise comparison - using the R package
121 *outliers* (Komsta, 2006). We intersected the set of 47,673 orthologous liver CREs with the
122 UCSC phastConsElements30wayPlacental track (Siepel et al., 2005), to assess whether

genomic regions characterized by conserved nucleotide sequence (i.e. phastCons elements) are significantly more associated to CREs detected as evolutionarily conserved in primates.

Analysis of features associated with evolutionary conservation of CREs

The following features were associated to each of predicted human CREs: nearest gene, distance from TSS, functional categories of genes, CRE category and histone mark (Table S2). Any human CREs without orthologous regions in other five species have been excluded from our analyses. To assess the correlation between the degree of conservation of a CRE and the number of cell types where the CRE is functional, we obtained publicly available data for DNase hypersensitivity sites (DHS) for over 200 cell types (ENCODE Project Consortium, 2012). For each CRE overlapping one or more DHS regions, we annotated the number of cell types where the specific CRE is putatively functional.

We estimated the correlation between the degree of conservation of CREs and the number of TFBSs by comparing our human consensus peaks with previously published HepG2 TF-binding profiles (ENCODE Project Consortium, 2012). Further, we quantified the proportion of putative primate CREs overlapping known transcribed enhancers (eRNAs) by using 43,011 known permissive transcribed enhancers (FANTOM5 Consortium, 2014). Similarly, for liver-specificity of human CREs analysis, we used coordinates of published liver eQTLs (Innocenti et al., 2011). We then selected all genes within 10 kb distance from evolutionarily conserved CREs for gene set enrichment analysis using GOrilla software (Eden et al., 2007; Eden et al., 2009). All genes found within 10 kb of any of the 47,673 orthologous CREs are used as a background for the enrichment test.

Known and *de novo* motif analysis

Genomic coordinates of orthologous regions were used to extract target sequences from the Ensembl references without MSA alignment gaps. All regions containing consensus peaks identified as human- and apes-specific and primate-conserved were used for the motif discovery and enrichment analysis. MEME-chip was used for known motif discovery and enrichment analysis using the Jaspar database (Bailey et al., 2009). We used DREME (Bailey, 2011). De novo motif identification was performed with AME (McLeay et al., 2010). Jaspar and Hocomoco (v10) databases were used as references to estimate similarities to known motifs. All motif discovery and enrichment analysis used default settings and parameters provided by the developers except for the maximum *de novo* motif discovery

157 threshold (changed from 1 to 1000 for maximum threshold). Shuffled input sequences were
158 used to estimate the background distribution of motifs.
159
160 **Overlap of transposable elements (TEs) with primate CREs**
161 We used Bedtools to overlap the RepeatMasker track for GRCh38 to the set of unique
162 human CREs that would overlap a TE for at least 25% of their length. TE enrichment
163 analysis was performed using the *TEAnalysis* pipeline with TE-analysis_Shuffle_bed v. 2.0,
164 setting 1000 replicates (https://github.com/4ureliek/TEanalysis; Kapusta et al., 2013). To
165 test the regulatory effect of enriched young TEs on primate gene expression, we performed
166 a differential gene expression analysis between Strepsirrhini (human, chimp, rhesus
167 macaque, marmoset) and Haplorrhini (bushbaby, mouse lemur) and quantified the number
168 of CREs associated to differential expressed genes that overlapped a TE younger than the
169 Haplorrhini-Strepsirrhini divergence.
170
171 **Analysis of SINE-VNTR-*Alu*s (SVA) TEs enriched in human CREs**
172 We intersected all known SVAs annotated in the human genome with all human consensus
173 peaks from our study. We used the same 25% overlap threshold as described above and
174 considered all human consensus peaks regardless of presence of orthologous regions in
175 the other species. The two SVA lists (overlapping and not overlapping the CREs,
176 respectively) were annotated for: the average distance from the closest TSS, functional
177 categories of associated gene, the average number of cell types with available DHS data,
178 the average number of TFBS overlapping the SVAs, and finally the average number of
179 TFBS within 10 kb up- and downstream of the SVAs. We used AME (McLeay et al., 2010)
180 to look for motifs enriched in the exapted SVAs, using the not exapted SVAs as a control.
181
182 **Luciferase reporter assay validation of *GRIN3A* and *JARID2***
183 To test for species- or clade-specific regulatory activity, we compared activity of two
184 predicted functional CREs with the empty pGL4.23 vector as a negative control. For
185 *GRIN3A* we PCR amplified the CRE (Table S6), and cloned the fragment into pGL4.23
186 using the NEB Gibson Assembly Kit. The *JARID2* CRE was synthesized by GenScript and
187 cloned into the same pGL4.23 vector. Cells were grown in DMEM high glucose (Gibco
188 #11965084) supplemented with 10% fetal bovine serum (FBS) (GE Healthcare Life
189 Sciences #SH3091003) containing antibiotic and antimycotic (Gibco #15240062) in a
190 humidified incubator with 5% CO_2 at 37°C. HepG2 cells were seeded in 48-well CellBIND

191 surface plates (Costar #3338) with 1.5 x 10^5 cells per well 24 h prior to transfection.
192 Transfection complexes were formed using 800 ng of each construct with 1 µL of TransIT-
193 LT1 transfection reagent (Mirus #MIR2304) and Opti-MEM (Gibso #31985070) in a total
194 volume of 27 µL, incubated for 20 min and then added to cells. After transfection, cells were
195 incubated for 24 h and were lysed in passive lysis buffer. To read firefly luciferase activity,
196 100 µL of LARII were added to 20 µL of cell lysate (from the dual-luciferase reporter assay
197 system from Promega #E1910). We read Luminescence for 2 seconds per well on a 96-well
198 compatible plate luminometer (ThermoFisher Luminoskan Ascent). The constructs were
199 tested using three vector preparations in three to four technical transfection replicates (9 to
200 12 measurements for for each construct). We normalized for transfection replicates effect
201 using a linear model:

202 *lm(log10(luciferase) ~ replicate + element*.

203

204 **Validation of the gene regulatory functionality of TE families**

205 HepG2 cells were cultured in DMEM + GlutaMAX (Gibco) supplemented with 10% Fetal
206 Bovine Serum (Gibco) and Normocin (InvivoGen). Transposable element constructs were
207 built by synthesizing (GenScript) the Dfam (Hubley et al., 2016) consensus sequence for
208 each element and cloning into the pGL3 Basic vector (Promega) with an added minimal
209 promoter (pGL3 Basic[minP]). pGL3 BASIC[minP] with no insert was used as the negative
210 expression control. pRL null (Promega) was the renilla control for transfection efficiency.
211 TAP2 cloned into the pGL3 Basic[minP] was the positive control. Confluent HepG2 cells in
212 opaque 96 well plates in 90ml of Opti-MEM (Gibco) were transfected according to the
213 Lipofectamine p3000 protocol (Invitrogen) with 100 ng of the luciferase containing plasmid,
214 1 ng of pRL null, 0.3 ml of Lipofectamine 3000, and 0.2ml of p3000 reagent in 10 ml of Opti-
215 MEM per well. The cells incubated in the transfection mixture for 24h hours then the media
216 was then changed to the regular FBS containing media for an additional 24 hours. Dual
217 Luciferase Reporter Assays (Promega) were started by incubating the cells for 15 mins in
218 20 ml of 1x passive lysis buffer. Luciferase and renilla expression were then measured
219 using the Glomax multi+ detection system (Promega). Luciferase expression values of the
220 transposable elements and TAP2 were standardized by the renilla expression values and
221 background expression values as determined by pGL3-Basic expression. Enriched motifs
222 were found by analyzing the Dfam (Hubley et al., 2016) consensus sequences of the TEs
223 found to have a regulatory ability significantly different from the pGL3 Basic[minP] empty

vector using the MEME Suite. TomTom (Gupta et al., 2007) was used to match binding site motifs in the Jaspar database to the enriched motifs found in our data.

Additional notes on analyses used throughout the project

All statistical analyses (DESeq2 analysis, Fisher's exact tests, logistic regressions, Spearman's correlations, Wilcoxon tests, General Linear Models, binomial test, and quantiles calculations) were performed using R v3.3.1. Figures were made with the package ggplot2 (Wickham, 2009) in R v3.3.1. Bedtools v2.25.0 (Quinlan et al., 2010) was used for overlap and closest feature/window analyses. All relevant scripts and pipelines are available online (https://github.com/ypar/cre_evo_primates.git).

Supplementary references

Aken, B.L., Ayling, S., Barrell, D., Clarke, L., Curwen, V., Fairley, S., Fernandez Banet, J., Billis, K., García Girón, C., Hourlier, T., et al. (2016). The Ensembl gene annotation system. Database 2016.

Andrews S., (2010). FastQC: a quality control tool for high throughput sequence data. Available online at: http://www.bioinformatics.babraham.ac.uk/projects/fastqc

Bailey, T.L. (2011). DREME: motif discovery in transcription factor ChIP-seq data. Bioinformatics *27*, 1653–1659.

Bailey, T.L., Boden, M., Buske, F.A., Frith, M., Grant, C.E., Clementi, L., Ren, J., Li, W.W., and Noble, W.S. (2009). MEME SUITE: tools for motif discovery and searching. Nucleic Acids Research *37*, W202-208.

Brown, C.D., Mangravite, L., and Engelhardt B. (2013) Integrative Modeling of eQTLs and Cis-Regulatory Elements Suggests Mechanisms Underlying Cell Type Specificity of eQTLs. Plos Genetics http://dx.doi.org/10.1371/journal.pgen.1003649

Dobin, A., Davis, C.A., Schlesinger, F., Drenkow, J., Zaleski, C., Jha, S., Batut, P., Chaisson, M., and Gingeras, T.R. (2013). STAR: ultrafast universal RNA-seq aligner. Bioinformatics *29*(1), 15–21.

Eden, E., Lipson, D., Yogev, S., and Yakhini, Z. (2007). Discovering Motifs in Ranked Lists of DNA Sequences. PLoS Comput Biol *3*, e39.

Eden, E., Navon, R., Steinfeld, I., Lipson, D., and Yakhini, Z. (2009). GOrilla: a tool for discovery and visualization of enriched GO terms in ranked gene lists. BMC Bioinformatics *10*, 1–7.

FANTOM Consortium and the RIKEN PMI and CLST (DGT) (2014). A promoter-level mammalian expression atlas. Nature *507*, 462–470.

261 Herrero, J., Muffato, M., Beal, K., Fitzgerald, S., Gordon, L., Pignatelli, M., Vilella, A.J.,
262 Searle, S.M.J., Amode, R., Brent, S., et al. (2016). Ensembl comparative genomics
263 resources. Database 2016.

264 Hinrichs, A.S., Karolchik, D., Baertsch, R., Barber, G.P., Bejerano, G., Clawson, H.,
265 Diekhans, M., Furey, T.S., Harte, R.A., Hsu, F., et al. (2006). The UCSC Genome Browser
266 Database: update 2006. Nucleic Acids Research *34*, D590–D598.

267 Hubley, R., Finn, R.D., Clements, J., Eddy, S.R., Jones, T.A., Bao, W., Smit, A.F.A., and
268 Wheeler, T.J. (2016). The Dfam database of repetitive DNA families. Nucleid Acids
269 Research *44*, D81-D89.

270 Gupta, S, Stamatoyannopoulos, J.A., Bailey, T.L., and Noble, W.S. (2007). Quantifying
271 similarity between motifs. Genome Biology *8*, R24.

272 Innocenti, F., Cooper, G.M., Stanaway, I.B., Gamazon, E.R., Smith, J.D., Mirkov, S.,
273 Ramirez, J., Liu, W., Lin, Y.S., Moloney, C., et al. (2011). Identification, Replication, and
274 Functional Fine-Mapping of Expression Quantitative Trait Loci in Primary Human Liver
275 Tissue. PLoS Genet *7*, e1002078.

276 Kapusta, A., Kronenberg, Z., Lynch, V.J., Zhuo, X., Ramsay, L., Bourque, G., Yandell, M.,
277 and Feschotte, C. (2013). Transposable Elements Are Major Contributors to the Origin,
278 Diversification, and Regulation of Vertebrate Long Noncoding RNAs. PLoS Genet *9*,
279 e1003470.

280 Komsta, L. (2006). Processing data for outliers. R News, 6(2), 10-13.

281 Landt, S.G., Marinov, G.K., Kundaje, A., Kheradpour, P., Pauli, F., Batzoglou, S., Bernstein,
282 B.E., Bickel, P., Brown, J.B., Cayting, P., et al. 2012. ChIP-seq guidelines and practices of
283 the ENCODE and modENCODE consortia. Genome Research *22*(9): 1813–1831.

284 Liao, Y., Smyth, G.K., and Shi, W. (2014). featureCounts: an efficient general purpose
285 program for assigning sequence reads to genomic features. Bioinformatics *30*, 923–930.

286 Liu, T. (2014). https://github.com/taoliu/MACS/wiki/Call-differential-binding-events.

287 Li, H. (2013) Aligning sequence reads, clone sequences and assembly contigs with BWA-
288 MEM. arXiv:1303.3997v1

289 Love, M.I., Huber, W., and Anders, S. (2014). Moderated estimation of fold change and
290 dispersion for RNA-seq data with DESeq2. Genome Biology *15*, 1–21.

291 McLeay, R.C., and Bailey, T.L. (2010). Motif Enrichment Analysis: a unified framework and
292 an evaluation on ChIP data. BMC Bioinformatics *11*, 1–11.

293 Melnikov, A., Murugan, A., Zhang, X., Tesileanu, T., Wang, L., Rogov, P., Feizi, S., Gnirke,
294 A., Callan, C.G., Kinney, J.B., et al. (2012). Systematic dissection and optimization of
295 inducible enhancers in human cells using a massively parallel reporter assay. Nat Biotech
296 *30*, 271–277.

297 Patwardhan, R.P., Hiatt, J.B., Witten, D.M., Kim, M.J., Smith, R.P., May, D., Lee, C.,
298 Andrie, J.M., Lee, S.-I., Cooper, G.M., et al. (2012). Massively parallel functional dissection
299 of mammalian enhancers in vivo. Nat Biotech *30*, 265–270.

Quinlan, A.R., and Hall, I.M. (2010). BEDTools: a flexible suite of utilities for comparing genomic features. Bioinformatics *26*, 841–842.

R Core Team (2016). R: A language and environment for statistical computing. R. Foundation for Statistical Computing, Vienna, Austria. URL https://www.R-project.org/.

Sharon, E., Kalma, Y., Sharp, A., Raveh-Sadka, T., Levo, M., Zeevi, D., Keren, L., Yakhini, Z., Weinberger, A., and Segal, E. (2012). Inferring gene regulatory logic from high-throughput measurements of thousands of systematically designed promoters. Nat Biotech *30*, 521–530.

Siepel, A., Bejerano, G., Pedersen, J.S., Hinrichs, A.S., Hou, M., Rosenbloom, K., Clawson, H., Spieth, J., Hillier, L.W., Richards, S., et al. (2005). Evolutionarily conserved elements in vertebrate, insect, worm, and yeast genomes. Genome Research *15*, 1034–1050.

Smedley, D., Haider, S., Durinck, S., Pandini, L., Provero, P., Allen, J., Arnaiz, O., Awedh, M.H., Baldock, R., Barbiera, G., et al. (2015). The BioMart community portal: an innovative alternative to large, centralized data repositories. Nucleic Acids Research *43*, W589–W598.

Villar, D., Berthelot, C., Aldridge, S., Rayner, T.F., Lukk, M., Pignatelli, M., Park, T.J., Deaville, R., Erichsen, J.T., Jasinska, A.J., et al. Enhancer Evolution across 20 Mammalian Species. Cell *160*, 554–566.

Wickham., H. (2009). ggplot2: Elegant graphics for data analysis. Springer-Verlag New York, 2009.

Yates, A., Beal, K.,Keenan, S., McLaren, W., Pignatelli, M., Ritchie, G.R.S., Ruffler, M., Tylor, K., Vullo, A. and Flicek, P. (2015). The Ensembl REST API: Ensembl Data for any language. Bioinformatics *31*(1): 143–145.

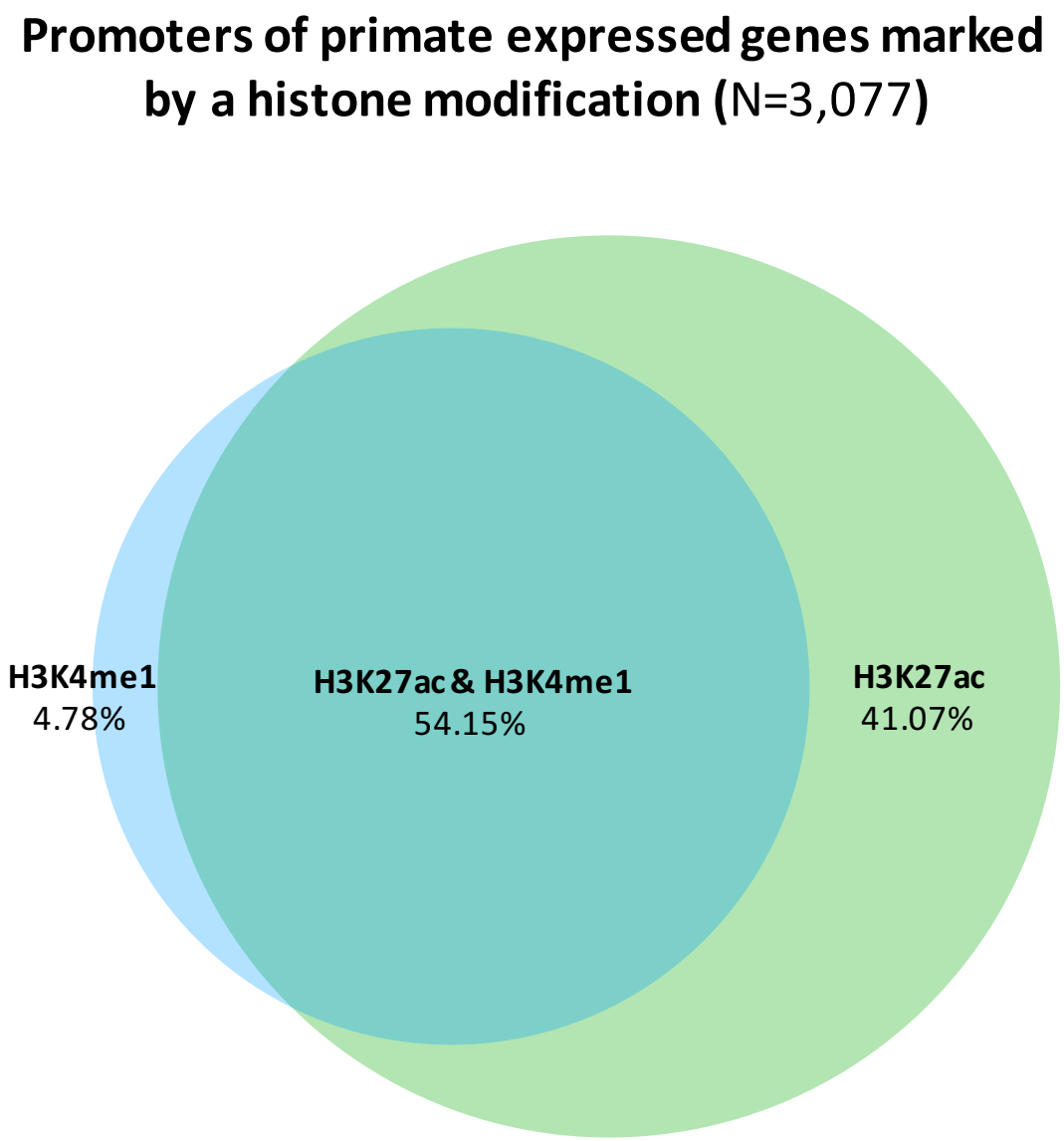

Figure S1: Promoters of genes that are expressed in primates are significantly histone modified. Venn diagram showing the distribution of histone marks on the promoters of genes that are expressed in the primate liver.

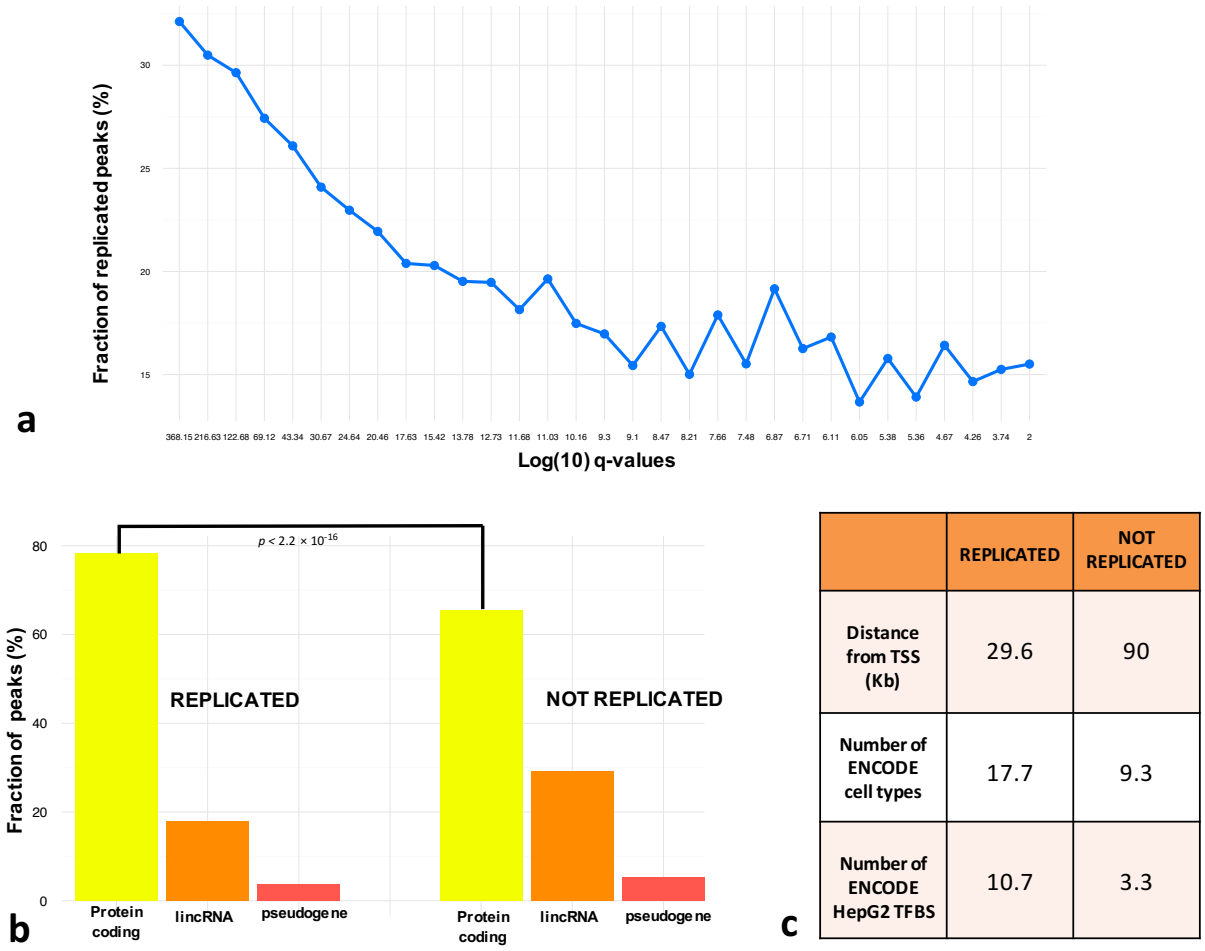

	REPLICATED	NOT REPLICATED
Distance from TSS (Kb)	29.6	90
Number of ENCODE cell types	17.7	9.3
Number of ENCODE HepG2 TFBS	10.7	3.3

Figure S2: Peaks bearing signatures of robust and broad regulatory activities are largely reproducible across studies. We compared our human H3K27ac data to a recent study focused on liver CREs in mammals (Villar et al., 2015). Overall, less than 40% of the peaks identified by Villar et al. (2015) overlapped one of our H3K27ac regions. Moreover, only 19% of the ENCODE HepG2 H3K27ac peaks were replicated in the Villar et al. (2015) dataset. We thus investigated possible features associated with ChIP-seq peak reproducibility.

(A) Peak discovery significance (q-value) is significantly correlated with cross-dataset reproducibility (logistic regression $p < 2.2\times10^{-16}$). (B) Replicated peaks are significantly more likely than non-replicated peaks to be associated with protein coding genes rather than with lincRNAs or pseudogenes (Fisher's exact test $p < 2.2\times10^{-16}$). (C) Replicated peaks are: 1) systematically closer to the nearest TSS (29.6 kb for replicated peaks, 90.8 kb for not replicated; Wilcoxon rank-sum test $p < 2.2\times10^{-16}$); 2) overlap chromatin accessible regions in significantly higher numbers of ENCODE cell types (an average of 17.7 cell types for replicated peaks and 9.3 cell types for unreplicated peaks; logistic regression $p < 2.2\times10^{-16}$); 3) contain a significantly higher number of transcription factor binding sites (TFBSs) per peak region as identified by ENCODE in HepG2 cells (10.7 TFBSs in the replicated peaks, 3.6 in the unreplicated; logistic regression $p < 2.2\times10^{-16}$).

Figure S3: Correlation of the normalized ChIP-seq read depths between human and marmoset. Human consensus peaks with orthologous in all the six species were split into two groups for this analysis: 1) regions with overlapping peaks present in both marmoset and human, and 2) regions with a peak present only in human. While human and marmoset normalized read counts were more highly correlated with each other in group 1 (Spearman's ρ = 0.67; $p < 2.2\times10^{-16}$), we found a nearly as strong correlation in group 2 (Spearman's ρ = 0.57; $p < 2.2\times10^{-16}$). These findings are consistent with the results of our differential histone modification state analyses, which demonstrated that only a small fraction of the 47,673 orthologous CREs (5.97%, FDR < 10%) are differentially modified, despite the fact that we had a much smaller total number of peak calls in the marmoset samples.

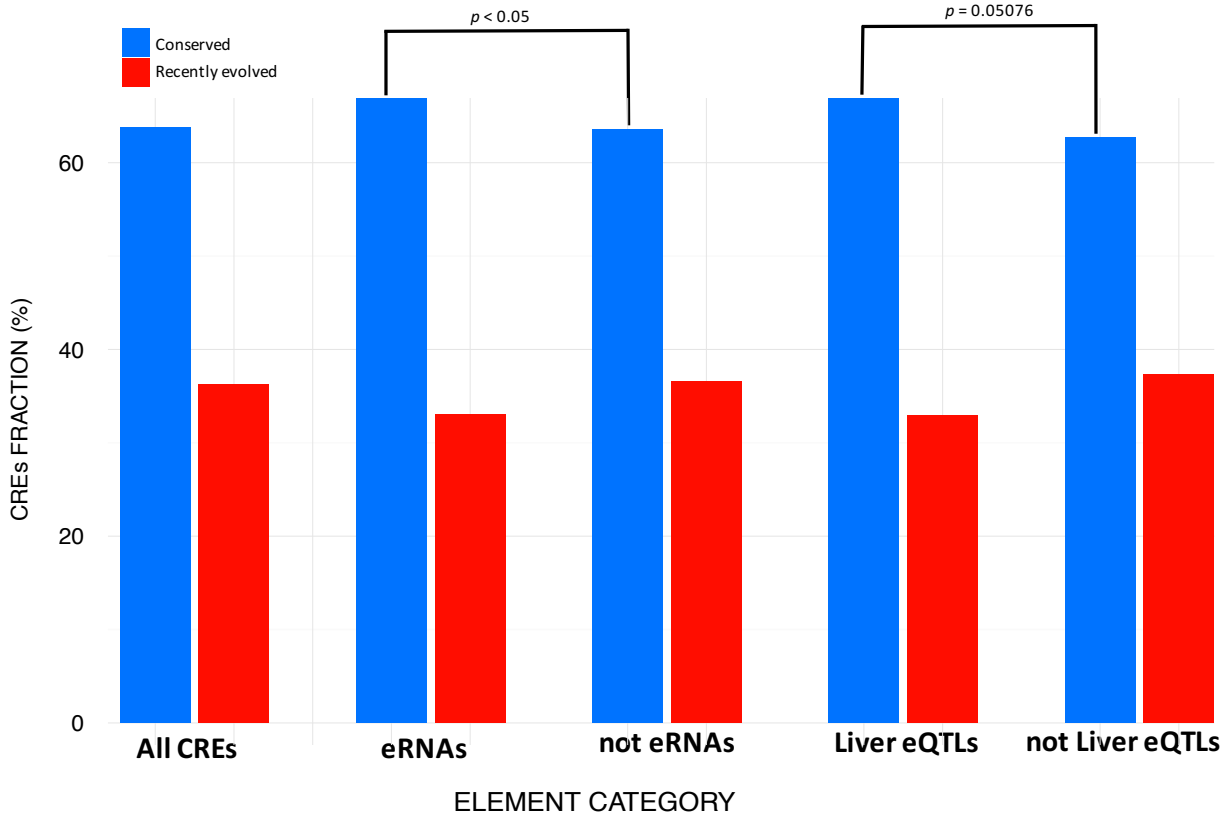

364
365 **Figure S4: Enhancers with signature of transcription are conserved.** Fraction of
366 conserved and recently evolved CREs with signature of transcription (eRNA) based on
367 FANTOM5 Consortium data. Fraction of conserved and recently evolved CREs with no
368 signature of transcription (eRNA) based on FANTOM5 Consortium data, Fraction of
369 conserved and recently evolved CREs overlapping and not overlapping liver eQTLs.
370 Specifically, predicted human CREs overlapped 500 eQTLs detected in a recent study on
371 human liver (Innocenti et al., 2011). We tested whether enhancers and promoters
372 overlapping liver eQTLs would lean toward being more conserved or more labile than a
373 random liver CRE, and we found that neither of these two conditions are satisfied (Fisher's
374 Exact Test p = 0.05076), as we show that liver eQTLs behave as “average” liver regulatory
375 elements.
376

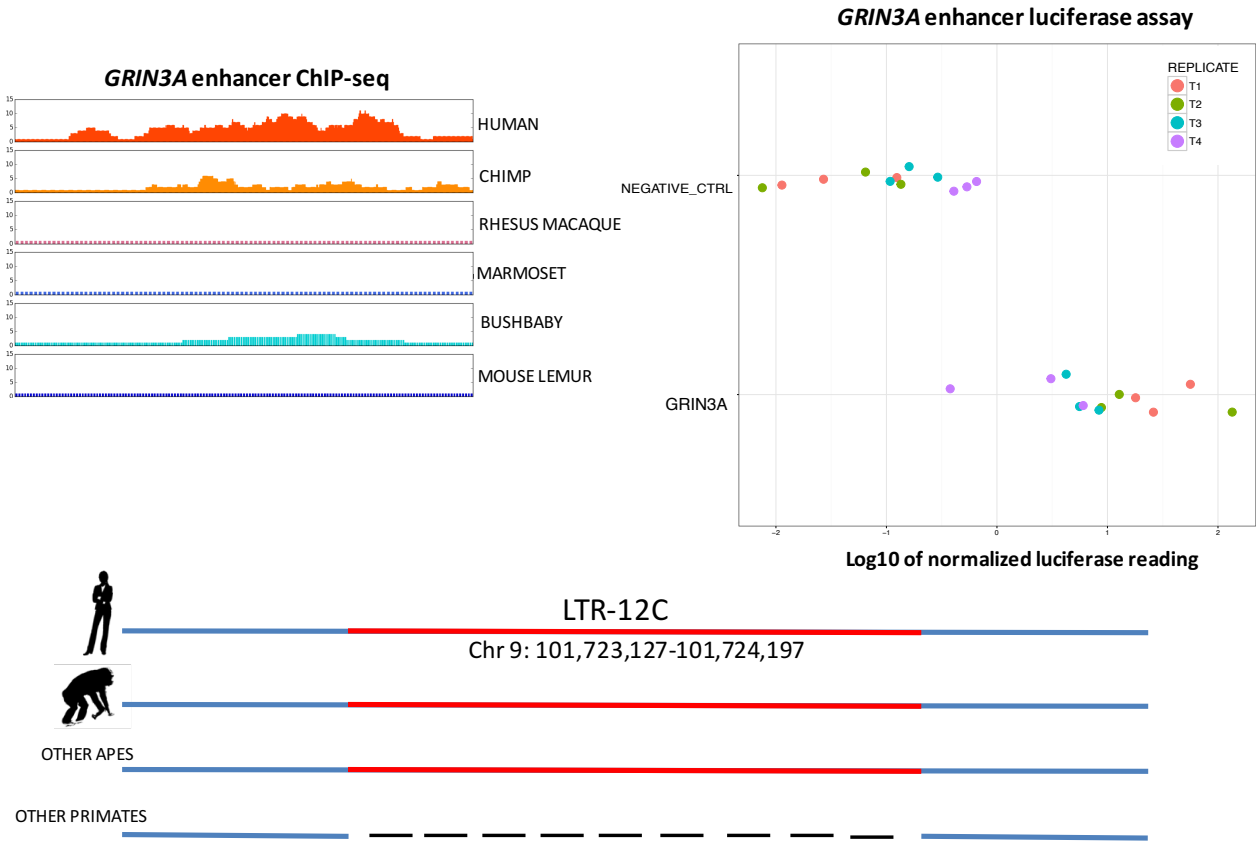

Fig S5: **Functional analysis on *GRIN3A locus*.** ChIP-seq read depth distributions and luciferase assays reporter activity for the CRE associated to *GRIN3A*.

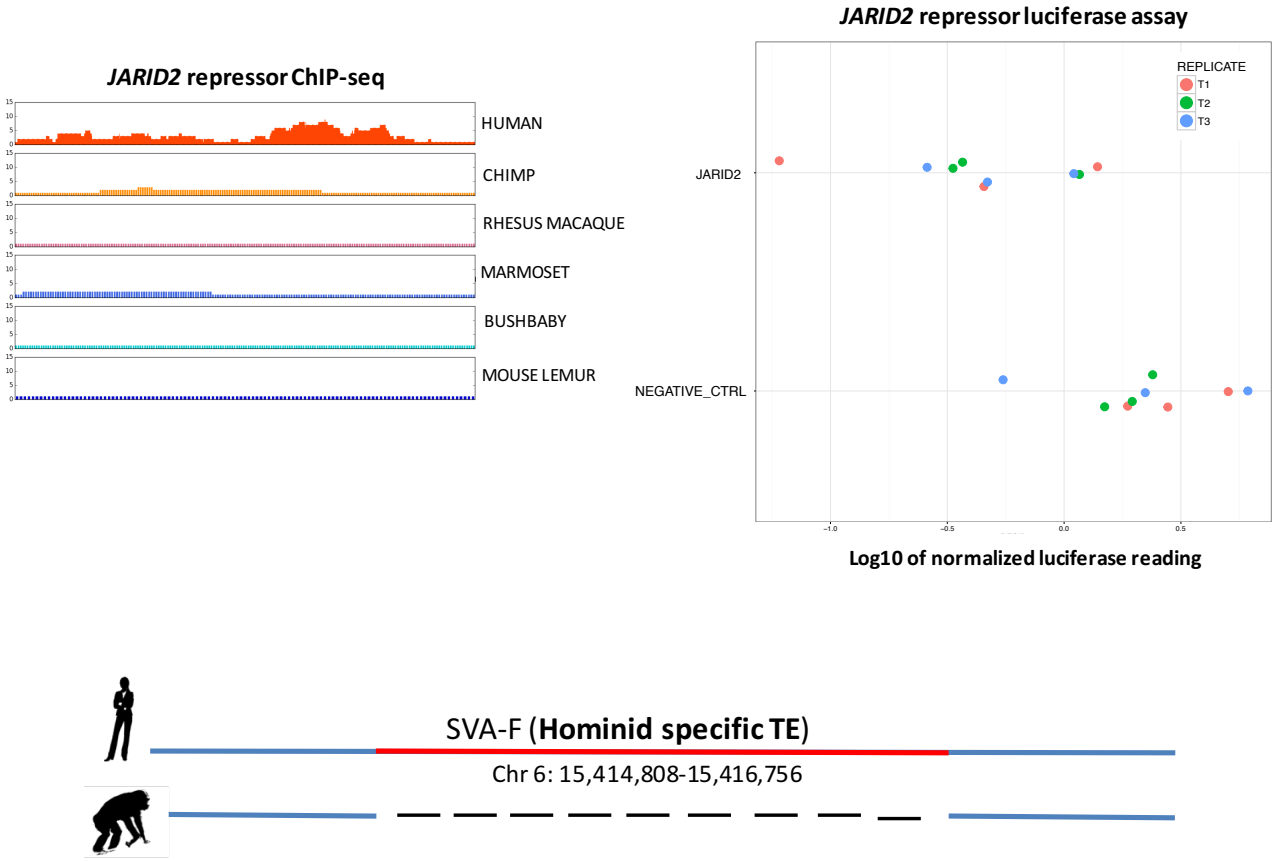

Fig S6: **Functional analysis on *JARID2 locus.*** ChIP-seq read depth distributions and luciferase assays reporter activity for the CRE associated to *JARID2*.

Figure S7: **Lineage specificity of enriched TEs.** Word-cloud representing the lineage specificity of the enriched TE families.